THE ASTROPHYSICAL JOURNAL, 458:543–560, 1996 February 20

LITHIUM PROCESSING IN HALO DWARFS, AND $T_{\rm eff}$, [Fe/H] CORRELATIONS ON THE SPITE PLATEAU

SEAN G. RYAN[1]
Anglo-Australian Observatory, P.O. Box 296, Epping, NSW 2121, Australia; and Department of Physics and Astronomy, University of Victoria, P.O. Box 3055, Victoria, BC, Canada V8W 3P6

TIMOTHY C. BEERS[2]
Department of Physics and Astronomy, Michigan State University, East Lansing, MI 48824

CONSTANTINE P. DELIYANNIS[3]
Center for Solar and Space Research, Center for Theoretical Physics, and Department of Astronomy, Yale University, P.O. Box 208101, New Haven, CT 06520-8101; and Institute for Astronomy, University of Hawaii, 2680 Woodlawn Drive, Honolulu, HI 96822

AND

JULIE A. THORBURN[4]
Yerkes Observatory, P.O. Box 258, Williams Bay, WI 53191-0258
Received 1995 June 7; accepted 1995 August 29

ABSTRACT

We present new Li data for seven halo turnoff stars chosen to test for diffusion. These are combined with data from the literature, and new effective temperatures and Li abundances are computed for the entire set on uniform temperature and abundance scales. We conclude that the effects expected of diffusion are not obvious in warm halo dwarfs, and uninhibited diffusion is unlikely to result in an initial Li abundance more than 0.1 dex higher than that inferred from nondiffusive models. (*Other* mechanisms for depleting Li, possibly by substantially larger amounts, are still possible.)

We consider the ongoing debate concerning the existence of correlations between the Li abundances for metal-poor stars and $T_{\rm eff}$ and overall metallicity, [Fe/H]. Molaro, Primas, & Bonafacio argue that previously reported slopes in the plateau as a function of these two variables (by Thorburn and Norris, Ryan, & Stringfellow) disappear when a subset of stars with temperatures based on Balmer line profiles is adopted. Upon closer examination of the Molaro et al. data and our own newly expanded data, we find that these correlations persist, but several points are worth noting: (1) suspected subgiants should be eliminated from the sample, (2) metallicity trends are evident only when stars of a wide range of metal abundances are included in the samples, especially the most metal-poor stars, (3) the tests must be performed in a multiple-regression environment (i.e., not when $T_{\rm eff}$ or [Fe/H] is considered the only independent variable), and (4) the results survive when robust regression methods are applied. Our current best estimate of the mean Li abundance as a function of $T_{\rm eff}$ and [Fe/H] is

$$A(\mathrm{Li}) = -0.09(\pm 0.30) + 0.0408(\pm 0.0052)T_{\rm eff}/100 + 0.111(\pm 0.018)[\mathrm{Fe/H}] \ .$$

The slopes of this relationship are consistent, within expected errors, with the results of Thorburn and Norris et al. The reported correlations appear to be real, in contradiction to the claim of Molaro et al.

We identify rare cases of well-observed stars with similar temperatures and metallicities which cannot have the same Li abundance; the contrast between G64−12, G64−37, and CD −33°1173 provides the best example. However, we defer our main discussion on a possible intrinsic spread in the Spite plateau to a separate paper.

Subject headings: diffusion — Galaxy: halo — stars: abundances

1. INTRODUCTION

Lithium is important in the study of stellar interiors, stellar evolution, and cosmology. Spite & Spite (1982) and subsequently numerous others have shown that halo dwarfs and subgiants with 5600 K $< T_{\rm eff} <$ 6300 K exhibit a nearly uniform plateau of Li abundances near $A(\mathrm{Li}) = 12 + \log N(\mathrm{Li})/N(\mathrm{H}) = 2.1$, whereas cooler halo stars are clearly depleted in Li. Although some suppose that the plateau abundance is the primordial value, stellar and/or Galactic processing may mean that this is not the case. It is vital that we understand what processes have modified Li in Population II stars.

The transport and/or destruction of Li may be followed in stellar models as they are evolved for a range of masses, metallicities, and ages, and surface abundances may be checked against observations for consistency. The predicted abundances depend on the physics in the models. Deliyannis, Demarque, & Kawaler (1990) studied Li depletion in "standard" stellar evolutionary models of halo stars, where we define standard models as those ignoring diffusion, mass loss, rotation, magnetic fields, and other physics not usually included in stellar evolution calculations. These models reproduced both the halo dwarf and subgiant observations with little Li depletion in the plateau. However, models with rota-

[1] sgr@aaoepp.aao.gov.au.
[2] beers@msuhep.pa.msu.edu.
[3] Hubble Fellow (Hawaii, Yale); Beatrice Watson Parrent Fellow (Hawaii); con@mozart.astro.yale.edu.
[4] Hubble Fellow; thorburn@yerkes.uchicago.edu.

tionally induced mixing triggered by instabilities related (in part) to angular momentum loss and transport deplete of order 90% of their initial Li (Deliyannis 1990; Pinsonneault, Deliyannis, & Demarque 1992; Yale models). If this loss occurs in halo stars, a very different primordial Li abundance must be inferred. It is clearly important to ascertain which stellar processes might be acting.

Diffusion has been held responsible for abundance anomalies in stars whose surfaces experience little mixing, bringing some elements to the surface in greater prominence whereas others sink from view. Surface convection is deeper in cooler stars and thus homogenizes their surface layers, so diffusion is more evident in hotter stars (spectral types A and earlier), provided they do not suffer other mixing (e.g., Michaud 1970). The peculiar abundances observed in Ap and Am stars are well known and are usually attributed to diffusion, with slow rotation and stabilizing magnetic fields suppressing additional mixing. The anomalous He abundances derived for blue horizontal branch stars and subdwarf O- and B-type stars are also ascribed to this, as are the abundances observed in HgMn stars.

Although halo dwarfs on the Spite plateau are much cooler than Ap and Am stars, stellar models in which diffusion is included predict a reduction in their surface Li abundance by as much as a few tenths of a dex, in which case the inferred primordial abundance would be correspondingly higher. If diffusion is not apparent in the observations, stellar modelers must ask, "Why not?" at which point we begin to learn more about the interiors of these stars; stellar processing of Li also reveals much about the internal details of the stars themselves. Stellar models, which we discuss in § 2, showed that the greatest difference between plateau models with and without diffusion was at higher temperatures, for which reason we concentrated our investigation on stars at the main-sequence turnoff. Our observations and the derived abundances are presented in § 3, supporting our statement of results in Deliyannis, Beers, & Ryan (1992) and Ryan (1993), finding no evidence for Li depletion arising from diffusion. We also revise Li abundances in the literature, putting the data from various workers onto uniform effective temperature and abundance scales, to reduce the scatter introduced to the overall sample by different treatments. The reassembled sample is discussed in § 4, with particular attention given to an examination of possible trends of Li abundance with temperature and metallicity. Our results are summarized in § 5.

2. STELLAR MODELS WITH AND WITHOUT DIFFUSION

"Diffusion" describes several competing processes which lead to chemical separation and includes gravitational settling, which tends to make heavier elements sink, thermal diffusion, which tends to push hydrogen toward lower temperatures (toward the surface), and radiative levitation, which provides additional buoyancy for selected species that retain at least one electron. For stars in which the mixing timescale is longer than the diffusion timescale, separation should occur. The effect of helium diffusion on globular cluster ages is one important astrophysical issue. Here we deal with a related issue, the effect on Li abundances. We refer the reader to Deliyannis & Demarque (1991) and references therein for further discussion of He diffusion and its connection with Li.

Evolutionary models of stars on the Spite plateau which include uninhibited diffusion of Li, for which radiative levitation is unimportant, show that this element sinks out of the surface convection zone (Deliyannis et al. 1990; Deliyannis & Demarque 1991). Owing to the inverse dependence of diffusion on the depth of the convective zone, and therefore dependence on effective temperature, diffusion diminishes the Li abundance of models more efficiently at the hot end of the plateau (>0.1 dex) than at the cool end (<0.1 dex). (Halo dwarfs cooler than about 5600 K have long been known to deplete for other reasons, and these will be discussed elsewhere.) The depletion of the hottest plateau stars is the signature we seek to reveal the effectiveness of diffusion in halo dwarfs.

The depth (by mass fraction, M_c) of the model convection zones near the turnoff is shallow (M_c of order 10^{-4} to 10^{-3}) and depends sensitively on opacities and the choice for mixing length, α. This can lead to widely differing degrees of Li diffusion, which can be constrained by Li data. Deliyannis et al. (1990) used existing Li observations to argue against those models predicting Li diffusion by several tenths dex at the turnoff. Larger opacities (possible because opacities are generally underestimated) and/or larger α (as possibly inferred from rotational and magnetic effects for advanced ages; Tayler 1986) result in both a deeper convection zone and thus less diffusion, fitting the data better. Although their standard Li isochrones provided the best fit to the Li data, Deliyannis et al. found *some* diffusive isochrones (including some with solar-calibrated α) that could not be ruled out and concluded that a maximum increase in the initial average plateau Li abundance of 0.1–0.2 dex was possible (owing to uninhibited diffusion alone).

Proffitt & Michaud (1991) computed Li and He diffusion simultaneously and also investigated the possible effects of nonconvective mixing on diffusion, using an ad hoc prescription for turbulence. They found that such homogenizing mixing could inhibit diffusion near the turnoff in better agreement with the data but would lead to even greater surface Li depletion through transport to depths where nuclear destruction occurs, resulting in higher inferred initial Li. Chaboyer & Demarque (1994) extended the Yale models by using updated opacities, model atmospheres, and nuclear reaction rates, and computing diffusion and rotationally induced mixing from instabilities simultaneously. They concluded that the observations of Thorburn (1994) argued against their pure diffusion models and proposed that rotational mixing was a successful way of inhibiting diffusion. Their combined diffusion + rotation models implied Li depletion by an order of magnitude (attributable almost exclusively to rotation), in good agreement with previous Yale models. While they found the [Fe/H] $= -2.3$ combined models to be in good agreement with the Li data, the -3.3 models were not.

Deliyannis et al. (1990) proposed that He diffusion could reduce globular cluster age estimates by as much as of order 25%, through its effects on the structure in the outer layers of stars near the turnoff. Whereas deep convection zones in cool dwarfs and in subgiants and giants would imply little He diffusion in these stars, in turnoff stars more efficient He diffusion results in larger model radii, or lower $T_{\rm eff}$. Matching the shape of a globular cluster color-magnitude diagram with a diffusive isochrone would then imply a lower age than matching with a standard isochrone. (See also Demarque, Deliyannis, & Sarajedini 1991; Proffitt & VandenBerg 1991; Chaboyer et al. 1992). In the absence of nonconvective mixing, Li diffusion would trace the He diffusion, and the improved definition of the Li morphology near the turnoff that we seek could provide constraints on age estimate reductions related to helium diffusion.

TABLE 1

ATMOSPHERIC PARAMETERS AND NEW Li DATA

Star	S/N	[Fe/H]	$T_{\rm eff}$	$W_{\rm Li}$	σ_W	$A_{\rm Li}$	Notes
BD −13°3442.....	230	−3.14	6180	19	1.0	2.06	
G13−9	200	−2.4	6200	26	1.0	2.21	= BD −04°3208
G41−41	150	−2.89	6260	20	1.5	2.12	= BD +09°2190
G64−37	150	−3.38	6290	16	1.5	2.04	
G84−29	270	−3.	6340	23	1.0	2.25	= BD +03°740
G186−26.....	150	−2.8	6200	<4	1.5	<1.36	
HD 84937	360	−2.20	6280	25	1.0	2.25	
	360	...	...	26.2	1.0	2.27	McDonald 2.7 m

3. OBSERVATIONS AND ABUNDANCES

3.1. *New Data*

To test for diffusion, we have obtained Li abundances for halo dwarfs at the hot end of the Spite plateau, since that is where diffusion is expected to be most evident. We selected suitably bright main-sequence turnoff stars and obtained high-dispersion spectra in the region of the Li doublet (6708 Å) with the Canada-France-Hawaii Telescope. We used the coudé spectrograph, 830 lines mm^{-1} grating, and PHX1 CCD, a 512 × 512, thick, coated Ford CCD with 20 μm square pixels. This setup yielded a dispersion of 0.095 Å $pixel^{-1}$ at a resolving power (FWHM) of 38,000. The data were reduced using IRAF.[5] The resulting spectra, with signal-to-noise ratios (S/Ns) between 100 and 200, are shown in Figure 1.

Equivalent widths, 1 σ photon noise errors, and other stellar parameters are provided in Table 1. One additional measurement we present here for the first time is for HD 84937, based on a spectrum taken with the McDonald Observatory 2.7 m telescope and coudé spectrograph at a resolving power around 100,000. The S/N and sampling of this spectrum result in an expected equivalent width error less than 1 mÅ. The selection of atmospheric parameters is discussed in § 3.3 in connection with Tables 2 and 3. To maximize the available sample, in the next subsection we include plateau dwarfs from the literature. For G186−26, we confirm the extreme Li deficiency already publicized by Hobbs, Welty, & Thorburn (1991); we discuss this star no further.

Besides the spectra listed in Table 1, we obtained *UBVRI* photometry following Ryan (1989) for the star CS 22958−042, yielding $V = 14.51$, $U-B = -0.24$, $B-V = 0.51$, $V-R = 0.29$, $R-I = 0.30$. Using color–effective temperature calibrations to be discussed in § 3.3, we derived an even lower effective temperature (5900 K) and Li abundance limit [A(Li) < 1.63] than Thorburn (1994), whose temperature estimate was based on Balmer lines, since photometry was not then available. However, these colors are not entirely consistent with those of a normal metal-poor main-sequence dwarf, as foreshadowed by Thorburn's classification of this star as a CH subgiant. Given its unusual characteristics, we feel justified in excluding it from further consideration in this paper.

3.2. *Revised* Li *Abundances from the Literature*

We combine our turnoff sample with cooler halo dwarfs to study the overall shape of the Spite plateau. We have searched the literature for Li observations of halo dwarfs having $T_{\rm eff} >$ 5500 K (since cooler dwarfs have destroyed much of their Li) and [Fe/H] ≤ −1.2. For the dwarf criterion we require $\log g > 3.5$ or that the star not have evolved beyond the turnoff in the dereddened $b-y, c1$ plane.

We reject subgiants from the sample because their higher masses mean that they spent their main-sequence lives at higher temperatures than those now observed and hence conform to a different Li evolution history (Deliyannis et al. 1990; Pilachowski, Sneden, & Booth 1993). Clearly, including the now cooler subgiants along with present-day dwarfs of similar temperatures would likely confuse any investigation of trends of Li abundance with temperature. Our sample is imperfectly defined, since a given star's gravity may not be known accurately, but completeness is not a significant issue to this topic. Near the main-sequence turnoff there is greater ambiguity over whether a particular star is a dwarf or subgiant, and when Strömgren photometry offered the only means of determining evolutionary status, we have refrained from eliminating stars with $b-y < 0.35$. Stars which we regard as *possible* subgiants but for which we lack sufficient evidence to completely exclude them are BD +02°4651, BD +17°4708, G18−54, G90−3, HD 3567, HD 24289, and HD 116064. For completeness, we note that among those we excluded as subgiants are the stars HD 132475, HD 134169, HD 140283, HD 160617, HD 166913, HD 189558, and BD +23°3912. We repeat from

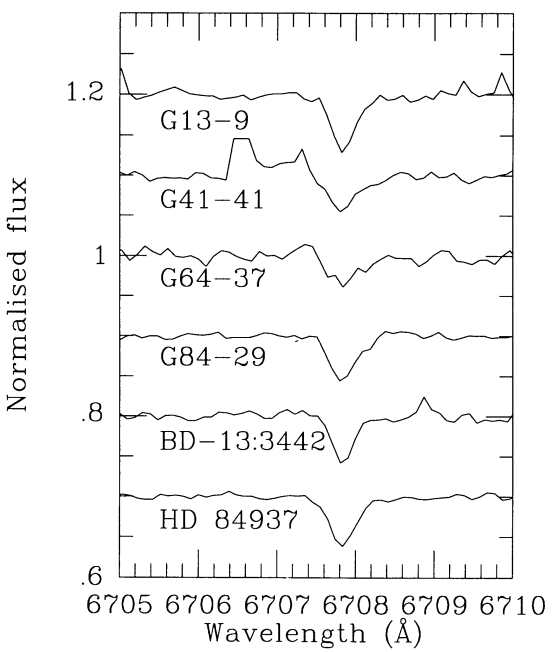

FIG. 1.—Li spectra for our program stars, offset by multiples of 0.1 continuum flux units.

[5] IRAF is distributed by Kitt Peak National Observatory, National Optical Astronomy Observatories, operated by the Association of Universities for Research in Astronomy, Inc., for the National Science Foundation

TABLE 2

LITERATURE DATA FOR METAL-POOR DWARFS

Star	[Fe/H]	W_{Li}	σ_W	T_{eff}	A_{Li}	References	Notes
BD +02°263	−2.35	37	2.4	5800	2.24	1	G71−33
BD +02°3375	−2.55	30	4.4	5820	2.00	2	G20−8
	−2.59	32	2.1	5850	2.04	3	
	−2.26	36	2.6	5850	2.13	4	
	−2.55	32	2.4	5890	2.23	1	
BD +02°4651[a]	−2.3	27	2.2	5794	1.92	5	G29−23
BD +03°740	−2.9	17!	1.5	6240	2.07	6	G84−29
	−3.13	21!	4.8	6140	2.13	2	
	−2.77	21!	3.7	6145	2.09	7	
	−3.0	19.3!	1.0	6400	2.15	8	
	−2.77	24!	2.4	6401	2.44	1	
	−3.	23!	1.0	6340	2.25	9	
BD +04°4551	−1.76	29	6.9	5670	1.88	2	
BD +07°4841	−1.2:	37	7.4	5900	2.24	2	G18−39
BD +09°352	−2.08	34	6.9	5870	2.12	2	G76−21
	−2.53	34	1.5	6099	2.41	1	
BD +09°2190	−2.89	18	3.4	6282	2.21	1	G41−41
	−2.89	20	1.5	6260	2.12	9	
BD +17°4708[a]	−2.0	25	1.5	5810	1.9	10	G126−62
	−1.95	25	3.7	5890	1.98	2	
BD +20°2030	−2.68	23	2.2	6321	2.37	1	G40−14
BD +20°3603	−2.2	28	3.1	5998	2.11	11	G183−11
	−2.3	27	3.0	6040	2.1	10	
BD +21°607	−1.6	25	2.8	5929	1.98	5	HD 284248
BD +24°1676	−2.59	26	2.2	6185	2.24	12	G88−32
	−2.60	28	2.9	6277	2.44	1	
BD +26°2606	−2.58	35	3.0	5980	2.24	2	G166−45
	−2.89	29	2.2	5950	...	12	
	−2.89	29	1.8	6053	2.29	1	
BD +26°2621	−2.82	20	2.9	6168	2.19	1	G166−54
BD +26°3578	−2.2	24	1.7	5998	2.01	5	
	−2.6	24	1.5	5830	1.8	10	
	−2.5	22.2	1.0	6250	2.11	8	
BD +28°2137	−2.16	27	2.2	6050	2.28	1	G59−27
BD +29°2091	−1.78	45	6.9	5670	2.10	2	G119−32
BD +34°2476	−2.3	22	2.2	6067	2.05	13	G165−39
	−2.3	<26		6110	<2.2	10	
	−2.3	23	2.0	6180	2.19	6	
BD +36°2964	−2.55	26	1.9	6072	2.26	1	G182−31
BD +39°2173	−2.23	25	2.1	6119	2.28	1	G115−34
BD +42°2667	−1.45	28	4.8	5960	2.12	2	G180−24
BD +42°3607	−2.12	47	4.5	5795	2.37	1	G125−64
BD +59°2723	−1.6	25	6.0	5830	1.95	2	G217−8
	−2.05	33	2.6	6050	2.24	4	
	−2.27	27	4.1	6056	2.28	1	
BD +71°31	−2.23	31	2.3	6156	2.42	1	G242−65
BD +72°94	−1.62	27	6.0	6160	2.22	2	
BD −04°3208	−2.38	24	2.1	6265	2.36	1	G13−9
	−2.4	26	1.0	6200	2.21	9	
BD −09°5746	−2.18	35	3.4	5892	2.29	1	G26−1
BD −10°388	−2.2	35	4.8	5980	2.18	2	G271−162
	−2.71	28	2.2	5955	...	12	
	−2.52	24	2.6	5950	2.00	4	
	−2.69	26	2.8	6135	2.30	1	
BD −13°3442	−3.14	30!	3.4	6168	2.39	1	
	−3.14	19!	1.0	6180	2.06	9	
CD −24°17504	−3.7	22[b]	4.1	6100	2.04	14	G275−4
	−3.70	21	3.4	6168	2.21	1	
	−3.70	19	2.3	6075	2.01	15	
CD −29°2277	−1.96	43	6.4	5704	2.25	1	W3314
CD −33°1173	−3.3	17[b]	2.7	6400	2.11	14	
	−3.29	12	2.4	6319	2.03	1	
	−3.29	10	1.5	6350	1.87	15	
CD −71°1234	−2.65	27	2.9	6268	2.41	1	
LP 56−75	−2.9	26[b]	3.4	6300	2.25	14	
	−2.93	25	3.6	6072	2.23	1	
LP 492−53	−2.58	25	3.4	5932	2.14	1	
LP 553−62	−2.55	15	3.2	6119	2.02	1	
LP 608−62	−2.7	23	4.5	6250	2.2	10	G48−29
	−2.66	23	4.5	6300	2.24	12	LP 608−62
	−2.66	21	2.6	6312	2.31	1	
LP 635−14	−2.80	24	3.9	6217	2.31	1	

TABLE 2—*Continued*

Star	[Fe/H]	W_{Li}	σ_W	T_{eff}	A_{Li}	References	Notes
LP 666−30	−2.50	28	3.9	6168	2.37	1	
LP 732−48	−2.46	17	2.9	6168	2.12	1	
LP 815−43	−3.2	27![b]	2.2	6350	2.32	14	
	−3.20	22!	2.1	6423	2.40	1	
	−3.20	15!	3.2	6350	2.06	15	
	...	13!	1.6	...	...	15	
LP 831−70	−3.4	26[b]	2.1	6000	2.06	14	
	−3.40	23	2.6	6119	2.22	1	
LP 916−15	−2.53	20	2.9	6119	2.16	1	
NLTT 0708−012	−2.48	34	3.4	5843	2.23	1	
CS 22186−017	−3.14	17	4.1	5978	1.96	1	
CS 22873−139A	−2.85	17	3.9	6423	2.28	1	
CS 22876−032A[c]	−3.80	15	1.9	6319	2.14	1	
	−4.21	15	2.3	6150	1.91	15	
CS 22884−108	−3.28	15	4.5	6319	2.14	1	
CS 22964−214	−3.29	16	4.1	6370	2.21	1	
CS 29499−060	−3.31	16	3.9	6217	2.10	1	
CS 29506−007	−3.10	24	4.8	6217	2.31	1	
CS 29527−015[d]	−3.4	<10	...	6250	<1.84	7	
	−3.50	<10	5	6319	<1.94	1	
G4−37	−2.75	20	2.8	6030	1.99	12	
	−2.78	19	3.4	6124	2.13	1	
G11−44	−2.37	29	3.1	5963	2.24	1	R 453
G18−54[a]	−1.33	35	2.6	5800	2.07	4	LP 640−75
G20−24	−2.14	20	3.4	6400	2.36	1	BD +01°3597
G21−22	−1.09	41	2.6	5700	2.08	4	LP 630−3
	−2.58	33	2.9	6093	2.39	1	same star?
G24−3	−1.63	29	2.6	5800	1.97	4	
G29−71	−2.40	28	2.9	5678	2.00	1	W1043
G59−24	−2.61	34	3.8	5990	2.24	12	W1447
	−2.63	37	2.6	5967	2.36	1	
G64−12	−3.5	25	5.0	6300	2.24	16	W1492
	−3.5	25	5.0	6072	2.08	16	
	−3.5	23	5	6350	2.23	17	
	−3.4	31[b]	4?	6325	2.34	14	
	−3.52	28	3.5	6205	2.27	7	
	−3.52	28	3.6	6197	2.37	1	
G64−37	−2.70	14	1.6	6376	2.15	1	R841
	−3.38	14	2.0	6350	2.03	15	
	−3.38	16	1.5	6290	2.04	9	
G66−9	−2.69	29	2.9	5650	1.99	1	LP 500−63
G75−56	−2.42	24	3.4	5993	2.17	1	
G88−10	−2.66	30	2.9	6012	2.29	1	
G90−3[a]	−1.93	44	2.6	5900	2.25	4	
	−2.48	44	2.9	5988	2.47	1	
G115−49	−2.21	38	3.4	5687	2.17	1	
G122−43	−2.76	34	2.2	5590	2.02	1	
G126−52	−2.48	26	3.6	6220	2.36	1	
G137−87	−2.72	30	2.8	5655	2.01	1	
G141−15	−2.78	30	3.2	5932	2.22	1	
G166−47	−2.49	25	3.2	6072	2.24	1	
G169−4	−2.72	17	2.4	6025	2.00	1	
G181−28	−2.66	31	3.1	6025	2.31	1	
G201−5	−2.66	25	2.2	6055	2.13	12	
	−2.66	22	2.8	6072	2.17	1	
G206−34	−2.89	27	2.5	6172	2.34	1	
G238−30	−3	33	5.0	5600	1.85	16	
	−3.03	29	2.9	5771	2.08	1	
G239−12	−2.50	24	3.1	6057	2.21	1	
G255−32	−2.62	30	2.9	5757	2.09	1	
G268−32	−3.50	27	3.9	5841	2.09	1	
HD 3567[a]	−1.2:	45	6.0	5950	2.35	2	
HD 16031	−2.2	28	2.2	5929	2.03	5	
HD 19445	−2.1	33	1.0	5728	2.00	11	G37−26
	−2.1	38	2.0	5810	2.1	10	+25°0495
	−2.2	35	3.0	5830	2.05	2	
	−2.0	33.2	1.0	5900	2.04	8	
	−2.12	32	1.2	5878	2.23	1	
	−2.20	34	1.0	5830	2.07	15	
HD 24289[a]	−2.19	49	3.4	5802	2.39	1	BD −4°680
	...	45	2.6	5570	2.00	4	G80−28
HD 74000	−1.8	25	3.4	6223	2.16	13	G43−3
HD 84937	−2.1	18!	2.2	6252	2.05	11	+14°2151

TABLE 2—*Continued*

Star	[Fe/H]	W_{Li}	σ_W	T_{eff}	A_{Li}	References	Notes
	−2.1	23!	1.0	6250	2.15	18	
	−2.1	20!	3.0	6200	2.1	10	
	−2.1	25!	1.0	6200	...	19	
	−2.5	24.5!	1.0	6250	2.15	8	
	−2.18	22!	2.5	6232	2.30	1	
	−2.20	25!	1.0	6280	2.25	9	
	−2.20	26.2!	1.0	6280	2.27	9	
HD 94028	−1.7	35	3.2	5794	2.09	11	G58−25
	−1.7	33	2.5	5860	2.1	10	
	−1.51	37	2.6	5800	2.09	4	
HD 108177	−1.9	35	7.3	5848	2.09	5	G13−35
	−1.9	29	1.5	5861	2.00	13	
	−1.9	<24	...	5900	<1.9	10	
	−1.67	36	3.4	5996	2.39	1	
HD 116064[a]	−2.39	30	2.5	5845	2.17	1	
HD 193901	−1.24	30	3.4	5690	1.95	2	
HD 194598	−1.6	27	1.0	5809	2.00	11	
	−1.6	29	2?	5808	2.00	5	
HD 201891	−1.4	23	1.0	5794	1.89	11	
	−1.4	27	1.5	5810	1.9	10	
	−1.4	27	4.8	5850	2.08	2	
	−1.5	23.4	1.0	5900	1.90	8	
HD 205650	−1.3	18:	2.2	5728	1.67:	5	cosmic ray?
HD 218502	−2.0	30	2.6	6000	2.16	4	
HD 219617	−1.4	42!	1.1	5662	2.10	11	
	−1.4	42!	...	5662	2.04	5	
	−1.4	43!	3.0	5820	2.2	10	
	−1.40	40!	3.2	5870	2.20	2	
	−1.50	36!	1.5	5870	2.13	15	

[a] Flagged in text as possible subgiant.

[b] We subtract 3 mÅ from these Spite & Spite 1993 equivalent widths before using them further, as described in the text.

[c] This spectroscopic binary has been treated as a turnoff and main-sequence composite. The equivalent widths and abundances refer to the turnoff primary.

[d] CS 29527−015 has not been used in the regression analysis because only an upper limit is available for its Li abundance.

REFERENCES.—(1) Thorburn 1994; (2) Rebolo, Molaro, & Beckman 1988; (3) Thorburn 1992; (4) Pilachowski et al. 1993; (5) Spite, Maillard, & Spite 1984; (6) Hobbs & Pilachowski 1988; (7) Thorburn & Beers 1993; (8) Hobbs & Thorburn 1994; (9) this paper; (10) Hobbs & Duncan 1987; (11) Spite & Spite 1982; (12) Hobbs & Thorburn 1991; (13) Spite & Spite 1986; (14) Spite & Spite 1993; (15) Norris et al. 1994; (16) Spite et al. 1987; (17) Rebolo, Beckman, & Molaro 1987; (18) Boesgaard 1985; (19) Pilachowski, Hobbs, & De Young 1989.

§ 3.1 that we have also excluded the CH subgiant CS 22958−042. We have also excluded stars with $A(\mathrm{Li}) < 1.5$ (such as G186−26) because these differ radically from plateau stars, for reasons that are not understood. The star HD 205650 appears only in Table 2, since its observation appears compromised by a cosmic ray; it is not utilized in the analysis. We carry the star CS 29527−015 in the tables but exclude it from our regression fits, since it has only an upper limit on its Li abundance. The two data tabulations for G21−22 are not in complete agreement, so we flag them as uncertain.

Systematic differences exist between the many Li studies owing to the adoption of various effective temperature scales and the use of different stellar models and abundance computations. As a first attempt to eliminate recognized systematics, we place all data onto common effective temperature and abundance scales.

The literature measurements are presented in Table 2, which includes our observations from Table 1. The columns contain the star name followed by metallicity, Li equivalent width, its 1 σ error, the effective temperature, and the derived Li abundance from each study referenced. The 1 σ errors are in most cases based on Cayrel's (1988) relationship between S/N and spectral resolution for an unresolved spectral line. However, we have replaced the instrumental resolution in that equation by the product of the resolution and 0.15 Å (combined in quadrature), to take account of the broad nature of the ^{7}Li doublet. This has the effect of giving larger error estimates than if we had treated the ^{7}Li line as unresolved. For the Pilachowski et al. (1993) sample, we have computed errors using their lowest S/N value. For the sample by Hobbs & Duncan (1987) which used a variety of instruments, we have instead adopted their own error estimates. Since most equivalent width measurements are quoted only to the nearest integer, in order to be a little conservative we set a limit of 1.0 mÅ as the highest precision claimed in any observation.

To permit further analysis of the available Li data, we combined the equivalent widths for which several measurements existed for a single star, but first we inspected the various data sets for differences which might reveal systematic errors in the original analysis, such as consistently high continuum placement or the like. The measurements of Thorburn (1994) formed the reference data in the comparison, since these are the most numerous from a single investigator and are of high internal precision. For most literature sources, either there were too few stars in common for a reliable comparison, or else the differences that existed could not confidently be ascribed to systematic errors amenable to transformation onto the Thorburn scale. The one exception to this was the data set of Spite &

TABLE 3

LITERATURE SAMPLE: PHOTOMETRY, TEMPERATURES, AND LITHIUM DATA

Star	$B-V$	$E(B-V)$	$R-I$	$b-y$	References	[Fe/H]	$T_{\rm eff}$	σ_T	$W_{\rm Li}$	σ_W	A(Li)	σ_A	Number of Observations	Notes
BD +02°263	0.49	0.01	0.35	...	1, 2	−2.4	5740	55	37	2.4	2.04	0.05	1	G71−33
BD +02°3375	0.45	0.01	0.35	0.354	1, 3, 4	−2.6	5840	38	33	1.3	2.06	0.03	4	G20−8
BD +02°4651[a]	0.45	0.02	0.33	0.339	2, 3, 4	−2.3	5990	44	27	2.2	2.08	0.05	1	G29−23
BD +03°740	0.36	0.03	0.30	0.309	1, 3, 4, 5	−2.9	6340	52	21!	1.0	2.21	0.05	6	G84−29
BD +04°4551	0.51	0.01	...	0.365	2, 4, 5	−1.8	5780	34	29	6.9	1.95	0.10	1	
BD +07°4841	0.46	0.02	0.32	0.345	1, 2, 4, 5	−1.2	6030	44	37	7.4	2.26	0.09	1	G18−39
BD +09°352	0.44	0.03	0.32	0.344	1, 2, 3, 4, 5	−2.3	6080	52	34	1.5	2.26	0.05	2	G76−21
BD +09°2190	0.39	0.02	...	0.305	1, 4	−2.9	6260	40	19	1.4	2.10	0.04	2	G41−41
BD +17°4708[a]	0.44	0.01	0.33	0.331	1, 2, 3, 4, 5	−2.0	5980	38	25	1.4	2.03	0.04	2	G126−62
BD +20°2030	0.38	0.02	...	0.308	1, 2, 4, 5	−2.7	6290	40	23	2.2	2.22	0.05	1	G40−14
BD +20°3603	0.44	0.01	0.30	0.320	1, 3, 4, 5	−2.3	6080	38	27	2.2	2.15	0.05	2	G183−11
BD +21°607	0.45	0.00	0.32	0.328	3, 4, 5	−1.6	5960	36	25	2.8	2.02	0.05	1	HD 284248
BD +24°1676	0.36	0.01	...	0.305	1, 4, 5	−2.6	6300	34	27	1.8	2.30	0.04	2	G88−32
BD +26°2606	0.43	0.02	0.33	0.333	1, 3, 4, 5	−2.7	6020	44	30	1.3	2.16	0.04	3	G166−45
BD +26°2621	0.41	0.01	...	...	1, 5	−2.8	6090	51	20	2.9	2.01	0.07	1	G166−54
BD +26°3578	0.39	0.02	0.33	0.313	1, 3, 4, 5	−2.4	6150	44	23	0.7	2.12	0.04	3	HD 338529
BD +28°2137	0.41	0.00	...	0.323	1, 4, 5	−2.2	6070	32	27	2.2	2.14	0.04	1	G59−27
BD +29°2091	0.50	0.00	0.34	0.376	3, 4, 5	−1.8	5720	36	45	6.9	2.13	0.07	1	G119−32
BD +34°2476	0.39	0.01	0.29	0.308	1, 3, 4, 5	−2.3	6220	38	23	1.5	2.16	0.04	2	G165−39
BD +36°2964	0.42	0.01	...	...	1	−2.6	6050	51	26	1.9	2.10	0.05	1	G182−31
BD +39°2173	0.40	0.00	...	...	6	−2.2	6120	50	25	2.1	2.14	0.05	1	G115−34
BD +42°2667	0.47	0.00	0.33	0.339	1, 3, 4, 5	−1.5	5880	36	28	4.8	2.01	0.07	1	G180−24
BD +42°3607	0.51	0.04	...	0.377	1, 5	−2.1	5850	59	47	4.5	2.25	0.06	1	G125−64
BD +59°2723	0.45	0.03	...	0.344	1, 3, 4, 5	−2.0	6050	49	29	2.1	2.16	0.05	3	G217−8
BD +71°31	0.39	0.00	...	0.309	1	−2.2	6170	32	31	2.3	2.28	0.04	1	G242−65
BD +72°94	0.41	0.06:	0.30	0.309	3, 5	−1.6	6460	82	27	6.0	2.42	0.11	1	
BD −04°3208	0.40	0.01	0.29	0.311	1, 2, 4	−2.4	6200	34	25	0.9	2.19	0.03	2	G13−9
BD −09°5746	0.49	0.03	0.33	0.362	1, 2, 4	−2.2	5940	52	35	3.4	2.17	0.06	1	G26−1
BD −10°388	0.42	0.01	0.32	0.326	1, 3, 4	−2.5	6040	34	27	1.4	2.11	0.03	4	G271−162
BD −13°3442	0.40	0.01	0.29	0.311	2	−3.1	6180	34	22!	3.9	2.12	0.08	2	
CD −24°17504	0.39	0.00	0.31	...	2	−3.7	6060	54	20	1.7	1.99	0.06	3	G275−4
CD −29°2277	0.51	0.00	0.36	0.365	2, 3, 4	−2.0	5660	36	43	6.4	2.06	0.07	1	W3314
CD −33°1173	0.36	0.00	0.28	...	2	−3.3	6260	54	12	1.2	1.89	0.06	3	
CD −71°1234	0.41	0.04	0.32	...	2	−2.7	6220	73	27	2.9	2.24	0.07	1	
LP 56−75	0.46	0.05	0.32	...	2	−2.9	6130	82	24	2.5	2.13	0.08	2	
LP 492−53	0.44	0.00	0.32	...	2	−2.6	5910	54	25	3.4	1.98	0.07	1	
LP 553−62	0.40	0.00	0.29	...	2	−2.6	6130	54	15	3.2	1.90	0.09	1	
LP 608−62	0.37	0.01	0.28	0.298	1, 5	−2.7	6300	34	22	2.3	2.20	0.05	2	G48−29
LP 635−14	0.43	0.05	0.31	...	2	−2.8	6260	82	24	3.9	2.22	0.09	1	
LP 666−30	0.41	0.02	0.31	...	2	−2.5	6150	59	28	3.9	2.21	0.07	1	
LP 732−48	0.41	0.02	0.31	...	2	−2.5	6150	59	17	2.9	1.98	0.08	1	
LP 815−43	0.38	0.04	0.30	...	2	−3.2	6380	73	18!	2.8	2.16	0.09	4	
LP 831−70	0.40	0.00	0.31	...	2	−3.4	6030	54	23	1.6	2.03	0.05	2	
LP 916−15	0.48	0.08	0.33	...	2	−2.5	6040	112	20	2.9	1.97	0.11	1	
NLTT 0708−012	0.51	0.05	0.35	...	2	−2.5	5910	82	34	3.4	2.13	0.08	1	
CS 22186−017	0.43	0.00	...	...	5	−3.1	5940	50	17	4.1	1.82	0.10	1	
CS 22873−139A	0.37	0.03	...	...	5	−2.9	6400	62	17	3.9	2.15	0.10	1	
CS 22876−032A	0.39	0.01	...	0.324	4, 5	−4.0	6230:	100	15	1.5	1.97	0.09	2	
CS 22884−108	0.50	0.14	...	...	5	−3.3	6280	180	15	4.5	2.01	0.18	1	
CS 22964−214	0.40	0.05	...	...	5	−3.3	6340	79	16	4.1	2.08	0.12	1	
CS 29499−060	0.38	0.00	...	...	5	−3.3	6180	50	16	3.9	1.97	0.10	1	
CS 29506−007	...	...	...	...	5	−3.1	6217:	100	24	4.8	2.19	0.11	1	Balmer $T_{\rm eff}$
CS 29527−015[b]	0.37	0.01	...	...	5	−3.5	6280	51	<10	5	<1.83	0.18	2	
G4−37	0.47	0.07	...	0.355	1, 4	−2.8	6130	92	20	2.2	2.04	0.09	2	
G11−44	0.44	0.00	0.32	0.335	1, 2, 4	−2.4	5930	36	29	3.1	2.07	0.05	1	R453
G18−54[a]	0.48	0.02	...	0.366	2, 4	−1.3	5912	40	35	2.6	2.14	0.04	1	LP 640−75
G20−24	0.46	0.08	...	0.362	1, 4	−2.1	6210	103	20	3.4	2.09	0.11	1	BD +01°3597
G21−22	0.53	0.11	0.34	0.381	1, 2, 4	−2.6	6230	140	37	1.9	2.40	0.11	2	LP 630−3
G24−3	0.47	0.03	...	0.363	1	−1.6	5960	49	29	2.6	2.09	0.05	1	
G29−71	0.53	0.02	...	0.399	1, 4	−2.4	5640	40	28	2.9	1.83	0.05	1	W1043
G59−24	0.43	0.00	...	0.333	1, 4	−2.6	5970	32	36	2.1	2.20	0.04	2	W1447
G64−12	0.38	0.02	0.29	0.305	1, 3, 4	−3.5	6290	44	27	1.8	2.29	0.05	5	W1492
G64−37	0.37	0.02	0.30	0.299	1, 2, 4	−3.0	6290	44	15	1.0	2.01	0.04	3	R841
G66−9	0.50	0.00	0.34	0.375	1, 2, 4	−2.7	5690	36	29	2.9	1.89	0.05	1	LP 500−63
G75−56	0.46	0.03	0.34	0.356	1, 2, 5	−2.4	5950	52	24	3.4	1.98	0.07	1	
G88−10	0.44	0.02	...	0.341	1, 4	−2.7	6010	40	30	2.9	2.14	0.05	1	
G90−3[a]	0.48	0.03	...	0.370	1, 4	−2.2	5880	49	44	1.9	2.24	0.04	2	
G115−49	0.50	0.00	...	0.371	1, 4	−2.2	5710	32	38	3.4	2.03	0.05	1	
G122−43	0.54	0.00	...	0.375	1	−2.8	5600	32	34	2.2	1.89	0.04	1	
G126−52	0.38	0.02	...	0.322	1, 4	−2.5	6240	40	26	3.6	2.24	0.06	1	
G137−87	0.51	0.02	0.37	0.396	1, 2	−2.7	5650	44	30	2.8	1.86	0.05	1	

TABLE 3—*Continued*

Star	$B-V$	$E(B-V)$	$R-I$	$b-y$	References	[Fe/H]	$T_{\rm eff}$	σ_T	$W_{\rm Li}$	σ_W	A(Li)	σ_A	Number of Observations	Notes
G141−15	0.54	0.10	...	...	1	−2.8	5910	133	30	3.2	2.07	0.12	1	
G166−47	0.41	0.00	...	...	1	−2.5	6040	50	25	3.2	2.06	0.07	1	
G169−4	0.47	0.04	...	...	1	−2.7	5960	70	17	2.4	1.84	0.08	1	
G181−28	0.44	0.02	...	...	1	−2.7	6000	56	31	3.1	2.00	0.06	1	
G201−5	0.41	0.00	...	...	1	−2.7	6040	50	24	1.7	2.06	0.05	2	
G206−34	0.43	0.05	...	0.340	1, 4	−2.9	6180	69	27	2.5	2.21	0.07	1	
G238−30	0.47	0.00	...	0.364	1	−3.0	5770	32	30	2.5	1.96	0.04	2	
G239−12	0.41	0.00	...	0.316	1	−2.5	6070	32	24	3.1	2.08	0.06	1	
G255−32	0.48	0.00	...	...	1	−2.6	5760	50	30	2.9	1.96	0.06	1	
G268−32	0.47	0.00	0.30	0.350	2, 4	−3.5	5910	36	27	3.9	2.02	0.07	1	706−7
HD 3567[a]	0.46	0.00	0.33	0.332	1, 3, 4	−1.2	5930	36	45	6.0	2.29	0.06	1	BD −09°122
HD 16031	0.44	0.01	0.32	0.322	1, 3, 4	−2.2	6020	38	28	2.2	2.12	0.04	1	BD −13°482
HD 19445	0.46	0.00	0.33	0.349	1, 3, 4	−2.1	5850	36	34	0.5	2.08	0.03	6	G37−26
HD 24289[a]	0.51	0.04	0.37	0.388	2, 4	−2.2	5780	61	47	2.1	2.20	0.05	2	G80−28
HD 74000	0.42	0.00	0.31	0.310	1, 3, 4	−1.8	6060	36	25	3.4	2.10	0.06	1	G43−3
HD 84937	0.40	0.01	0.27	0.303	1, 3, 4	−2.1	6280	38	24!	1.2	2.23	0.04	8	BD +14°2151
HD 94028	0.47	0.00	0.31	0.342	1, 3, 4, 5	−1.7	5930	36	35	1.6	2.16	0.03	3	G58−25
HD 108177	0.43	0.00	0.32	0.325	1, 3, 4	−1.8	5990	36	32	1.3	2.16	0.03	3	G13−35
HD 116064[a]	0.47	0.01	0.33	0.349	3, 4, 5	−2.4	5880	36	30	2.5	2.05	0.05	1	BD −38°8457
HD 193901	0.55	0.00	0.33	0.377	1, 2, 4	−1.2	5710	36	30	3.4	1.90	0.05	1	BD −21°5701
HD 194598	0.49	0.00	0.31	0.348	1, 3, 4	−1.6	5900	36	28	0.9	2.03	0.03	2	BD +09°4529
HD 201891	0.51	0.00	0.33	0.357	1, 3, 4, 5	−1.4	5800	36	24	0.6	1.87	0.03	4	BD +17°4519
HD 218502	...	0.01:	...	0.315	5	−2.0	6160	38	30	2.6	2.25	0.05	1	
HD 219617	0.48	0.00	0.33	0.341	1, 4	−1.4	5870	36	40!	1.3	2.18	0.03	4	BD −14°6437

[a] Flagged in text as possible subgiant.

[b] CS 29527−015 has not been used in the regression analysis because only an upper limit is available for its Li abundance.

REFERENCES.—(1) Carney 1979, 1989; Carney et al. 1994. (2) Ryan (1989). (3) Cayrel de Strobel et al. 1992; $R-I$ colors on the Kron system were transformed to the Cousins system using the transformation of Bessell 1979. (4) Schuster & Nissen 1989; Schuster, Parrao, & Contreras Martinez 1993. (5) See original Li papers and references therein.

Spite (1993), whose six measurements were systematically larger than those of Thorburn by 3.0 mÅ with σ (Spite & Spite—Thorburn) = 1.8 mÅ.[6] Consequently, we have transformed the original measurements of Spite & Spite (1993), given in Table 2, onto Thorburn's scale before combining these and other data into Table 3. This procedure concerns only six stars, and even then their abundances are barely altered, since other measurements also contribute to the mean equivalent width. None of the important conclusions of the paper are sensitive to the transformation.

If we believed that all the errors were Gaussian (attributable only to photon noise), we would weight each measurement by its value for the variance. However, errors are sometimes non-Gaussian, being affected by cosmic-ray strikes, inappropriate flat-fielding, poor subtraction of the background, bias or scattered light, and possibly poor continuum fitting (though this is not a major problem in the red spectra of these metal-poor stars). Consequently, we weight each observation by its standard deviation rather than its variance. The weighted mean equivalent widths are tabulated in Table 3 along with the standard errors in the mean, calculated from the σ values of the actual measurements. However, in a few cases discussed in § 4.3, the scatter of individual measurements significantly exceeds the stated individual errors, and for these we give the standard error of the mean computed from the scatter; these cases are flagged in Tables 2 and 3 by an exclamation point following the equivalent widths.

[6] We emphasize that this comparison does *not* indicate that the Spite & Spite data are inferior to the remainder in the study. Rather, its *random* errors are sufficiently *small* compared to 3.0 mÅ that we felt confident assigning the offset relative to Thorburn's measurements to systematic differences.

3.3. *A Uniform* Li *Abundance Analysis for the Combined Sample*

Photometric colors have been taken from the Li papers, from the photometric data of Carney (1979, 1989), Carney et al. (1994), Ryan (1989), and Schuster & Nissen (1988, 1989), and from the compilation by Cayrel de Strobel et al. (1992). In Table 3 we tabulate observed $B-V$, $R-I$, and $b-y$ colors, since they are available for a large fraction of the sample. Reddening estimates from the literature for $B-V$ and $b-y$ were averaged, allowing for the ratio $E(b-y) = 0.7E(B-V)$. In the subsequent reanalysis, the color excesses were applied to all three colors, using $E(R-I) = 0.8E(B-V)$.

We have used the colors and metallicities to recompute effective temperatures on a uniform scale. This scale is almost guaranteed to be incorrect, but using one incorrect (but consistent) scale makes it easier to compare stars than when different workers have used different incorrect scales. We used the color–effective temperature scale of Magain (1987, eq. [15]) for $b-y$, viz.,

$$T_{\rm eff} = 8330 - 7040(b-y)(1 - 0.099 \times 10^{[{\rm Fe/H}]}) ,$$

and for $R-I$ we use

$$T_{\rm eff} = 8700 - 8770(R-I) ,$$

following Buser & Kurucz (1992) and Bell & Oke (1986).

Owing to the metallicity sensitivity of $B-V$, this color is more difficult to work with. We have consulted the scales of VandenBerg & Bell (1985), Magain (1987), Buser & Kurucz (1992), and Bell & Oke (1986), and we interpolate within the grid points given in Table 4. These three colors give reasonably consistent temperatures, with very good agreement between $B-V$ and $b-y$ temperatures but somewhat more scatter

TABLE 4

ADOPTED $B-V$ COLORS

	[Fe/H]		
$T_{\rm eff}$	−1	−2	−3
6500.....	0.35	0.33	0.32
6000.....	0.46	0.43	0.415
5500.....	0.60	0.56	0.54

NOTE.—The tabulated numbers are $B-V$ colors for the metallicities in the column headings.

against $R-I$, since the sensitivity of $T_{\rm eff}$ to typical photometric errors is greater (see below). Since $B-V$ and $b-y$ measure similar (though not identical) spectral regions, agreement between these two is not so surprising. The $R-I$ temperatures exceed the $B-V$ temperatures on average by perhaps 50 K for the cooler half of the sample, but the systematics are too marginal to justify adjusting the scales further. We adopt an unweighted mean of the available temperatures, rounded to the nearest 10 K. Two exceptions are CS 22876−032A and CS 29506−007. For the first, we adopt the temperatures inferred for the primary as referenced in Table 2, and for the second we adopt the estimate based on its Balmer line profile, again as in Table 2.

The uncertainty in each $T_{\rm eff}$ was computed as follows. The 1 σ error in each observed color is probably of order 0.01 in $B-V$ and $R-I$ (Ryan 1989, Table 2) and perhaps 0.005 in $b-y$ (Schuster & Nissen 1988), corresponding to effective temperature errors of 50 K, 90 K, and 35 K. In addition, each reddening estimate is uncertain by possibly half the reddening value, i.e., 2 $\sigma = 0.5E(B-V)$. We combine the errors for whichever of these four sources contribute, giving the 1 σ estimate in Table 3. We arbitrarily adopt 100 K as the 1 σ error in the Balmer line temperature.

Systematic errors arising with the particular choice of color–effective temperature transformations are likely. These can be in the nature of a zero point error, a temperature-dependent (scale) error, and an incorrect metallicity dependence. The first will shift all stars the same amount, but the second and third can produce different effects for different stars even within our homogenized sample. Because $R-I$ is less sensitive to metallicity in plateau stars, it minimizes the third of these error sources. The $B-V$ calibrations referenced above can differ by up to 200 K for a given color and metallicity; errors of 50 K arising from the calibrations certainly would not be surprising.

We have not attempted to adjust [Fe/H] values to the new effective temperature scale, owing to the diverse techniques used to determine the metallicities in the first place, and because precise metallicities, though desirable, are not crucial to our study. Typical errors in the determination of [Fe/H] are expected to be of the order 0.2–0.3 dex, which introduce errors of $\leq$0.01 dex into the estimate of A(Li) abundance. Errors in [Fe/H] do, of course, add to the scatter of points in the presence of a metallicity-dependent A(Li) trend. A trend of 0.1 dex in A(Li) per dex in [Fe/H] would introduce additional scatter of only 0.02–0.04 dex owing to these [Fe/H] errors, which is less than most of the 1 σ uncertainties in A(Li) listed in Table 3 and the A(Li) ranges evident in Figures 3 and 5.

A lithium abundance computation requires a measured equivalent width, adopted atmospheric parameters for the star under consideration, of which the effective temperature is the most important, and an atmospheric model. Even then, abundances can be computed using a variety of techniques. In order to eliminate differences between studies, especially the use of different temperatures and atmospheres, we have used the revised effective temperatures and combined equivalent widths to recompute abundances, presenting the new results in Table 3. Abundances were computed using the procedure detailed in Norris, Ryan, & Stringfellow (1994), computing synthetic spectra for Bell (1981) models, using four ^{7}Li components, and measuring the equivalent width of the synthesized line. These computations are presented as Figure 2 and Table 5. Gravity has a negligible effect on the Li line over the range of interest. At 5500 K the log g = 4.0 models yield abundances only 0.01 dex higher than those with log g = 4.5 (for a given equivalent width), and at higher temperatures the effect is even smaller. The adopted stellar metallicity affects the abundances slightly more; at 5500 K, models with [Fe/H] = −2.0 yield Li abundances 0.035 dex higher (at fixed equivalent width) than models at [Fe/H] = −1.0, but at 6500 K the effect is smaller and in the opposite sense, with −2.0 models giving abundances 0.015 dex lower than the −1.0 models. Note, however, that these offsets are valid only for the models used, as we discuss more fully below. Linear interpolation at constant equivalent width between two isotherms in Figure 2 is adequate to obtain abundances. For stars with −2.0 < [Fe/H] < −1.0, we interpolate between the curves of growth for these two metallicities; for [Fe/H] < −2.0, we adopt the abundances for models with [Fe/H] = −2.0. We adopt log g = 4.5 for stars cooler than 6000 K and log g = 4.0 for stars hotter than 6000 K. Thermal broadening greatly exceeds microturbulence for this light atom, rendering microturbulence relatively unimportant. We have used ξ = 1.0 in all computations.

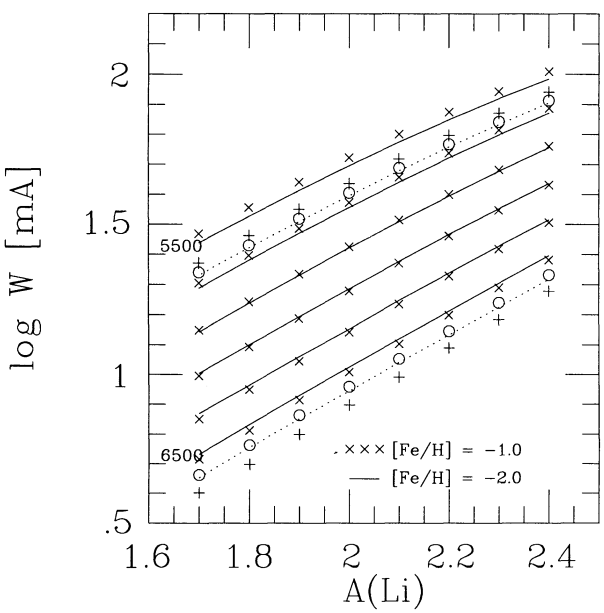

FIG. 2.—Li equivalent widths computed for effective temperatures at 200 K intervals between 5500 and 6500 K, and for A(Li) between 1.70 and 2.40. Solid lines and crosses correspond to [Fe/H] = −2.0 and −1.0 using the models of Bell (1981). Dotted lines, plus signs, and circles give the curves at 5500 K and 6500 K for Kurucz (1993) models at [Fe/H] = −2.0, −1.0, and −3.0, respectively. The Kurucz models are hotter in the line-forming regions than the Bell models for a given effective temperature, leading to higher inferred Li abundances for a given equivalent width. Linear interpolation in effective temperature and in log equivalent width is permissible.

TABLE 5

Li EQUIVALENT WIDTHS (mÅ) FOR BELL MODELS

	A(Li)							
MODEL	1.70	1.80	1.90	2.00	2.10	2.20	2.30	2.40
6500/4.0/−1.....	5.2	6.5	8.2	10.2	12.7	15.8	19.5	24.1
6300/4.0/−1.....	7.1	8.9	11.1	13.9	17.2	21.3	26.2	32.1
6100/4.0/−1.....	9.9	12.4	15.4	19.0	23.5	28.9	35.3	42.8
5900/4.5/−1.....	14.1	17.5	21.6	26.6	32.7	39.8	48.1	57.7
5700/4.5/−1.....	20.2	24.9	30.6	37.4	45.4	54.7	65.3	77.1
5500/4.5/−1.....	29.4	36.0	43.7	52.8	63.2	74.9	87.7	102.
6500/4.0/−2.....	5.4	6.8	8.5	10.6	13.2	16.3	20.2	24.9
6300/4.0/−2.....	7.4	9.2	11.5	14.2	17.7	21.8	26.8	32.8
6100/4.0/−2.....	10.1	12.6	15.6	19.3	23.8	29.3	35.7	43.3
5900/4.5/−2.....	13.9	17.3	21.4	26.4	32.3	39.3	47.6	57.0
5700/4.5/−2.....	19.4	23.5	29.5	36.0	43.7	52.7	62.9	74.4
5500/4.5/−2.....	27.4	33.6	41.0	49.6	59.5	70.7	83.1	96.5

The newly computed abundances are given in Table 3, along with 1 σ errors incorporating the propagated error in equivalent width and 0.08 dex per 100 K of random error in effective temperature. The subsequent column indicates how many Li observations contributed to the result.

As noted above, one significant difference between analyses is the choice of stellar atmospheric models. This is particularly true of the newer Kurucz (1993) models, where temperatures in the line-forming regions may be up to 200 K higher than those in older models (Kurucz 1989) with the same effective temperature and gravity. Consequently, these models require higher Li abundances to match a given line strength than did older models with cooler line-forming layers. Such a difference led to the generally higher abundances (by of order 0.1–0.2 dex) obtained by Thorburn (1994) compared to several earlier works. Which models should we believe? Probably none. We compute abundances using one set for all observations and remain alert to likely revisions of systematics in the future. (See Kurucz 1995 for a discussion of potentially large-scale revisions.) In Figure 2, along with the curves of growth for the Bell models, we illustrate the change at effective temperatures of 5500 K and 6500 K of adopting the Kurucz (1993) models. The dotted lines give the curves of growth for these temperatures at [Fe/H] = −2.0, which can be compared with the upper and lower solid curves for Bell models, and the plus signs give the calculations for [Fe/H] = −1.0, to be compared with the crosses for Bell models. The open circles show the Kurucz models at [Fe/H] = −3.0 and differ little from the −2.0 models. The Kurucz models would produce Li abundances 0.08 dex higher at 6500 K and 0.15 dex higher at 5500 K. The choice of models thus influences the slope with effective temperature derived for the Spite plateau, quite apart from any scale errors in the color-temperature transformations. Changing from Bell to Kurucz models would reduce it by 0.007 dex per 100 K, though this is still much less than the roughly 0.03 dex per 100 K slope measured by Thorburn (1994) and Norris et al. (1994). (See also Thorburn 1994 concerning model-dependent effects.)

The abundances discussed here have been computed in LTE. Carlsson et al. (1994) compute small non-LTE effects for Li in plateau stars, but these are not capable of eliminating the observed trends with $T_{\rm eff}$ and [Fe/H]. Adoption of their corrections would reduce the slope with $T_{\rm eff}$ by only 0.008 dex per 100 K at [Fe/H] = −2.0 and by slightly less at lower metallicities. Furthermore, there is effectively no difference between the non-LTE corrections at [Fe/H] = −2.0 and −3.0, offering no hope of eliminating the observed trends with metallicity.

4. DISCUSSION OF Li ABUNDANCES

4.1. *Trends with Effective Temperature and Metallicity*

In Figure 3 we show the Li abundances of the homogenized sample of stars for which we have eliminated scatter attributable to different effective temperature scales and Li abundance computations. In Figures 3*b*–3*d* we divide the sample into three similar-size groups based on metallicity: [Fe/H] > −2.25, −2.75 < [Fe/H] < −2.25, and [Fe/H] < −2.75. These subsamples have median metallicities −1.8, −2.6, and −3.1, respectively. The error bars shown are 1 σ errors. Because errors in A(Li) are correlated with errors in effective temperature, the error boxes are in reality skewed with slope 0.08 dex per 100 K. The most metal-poor group is concentrated around the turnoff owing to the luminosity bias in the searches for extremely metal-poor stars. The potential influence of this bias on the interpretation of correlations between A(Li), temperature, and metallicity underscores the need for additional observations of extremely metal-poor stars from farther down the main sequence. The solid sloping lines in these figures come from our best fit, to be discussed in § 4.1.2, evaluated at the median metallicity of each bin.

Two features discussed by Thorburn (1994) and Norris et al. (1994) are trends with effective temperature, at a level of 0.030 dex per 100 K, and with [Fe/H], at a level of 0.1 dex per dex. Both trends can be studied better with the present sample, which has been placed on a uniform effective temperature and abundance scale and which includes all available observations; Thorburn's sample had only three stars with [Fe/H] > −2.0, whereas the present sample includes 19 above this limit, and the study by Norris et al. used data straight from the literature without the benefit of homogenization. Below, we first consider the results of a "standard" weighted least-squares analysis, under the somewhat optimistic assumption that our derived errors in the Li abundances are purely statistical in nature; i.e., that there exist no unrecognized systematics within the data. This is followed by several examinations of the results using an unweighted least-squares analysis and a reweighted least-squares technique, based on the least median of squares (Rousseeuw & Leroy 1987), which does *not* consider the error in estimation of Li abundance in the calculation of the regression coefficients but obtains a resistant fit to the main trends of

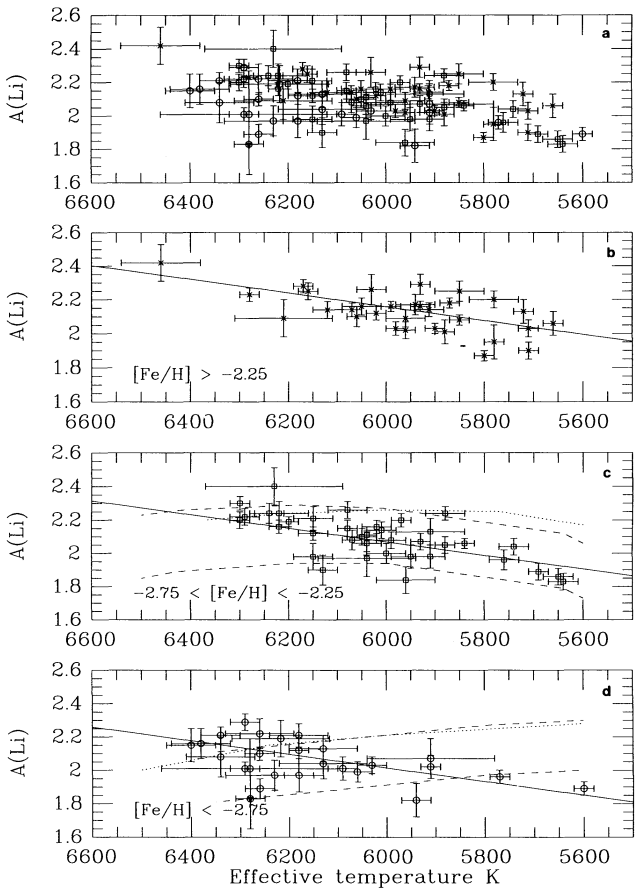

FIG. 3.—Li abundances recomputed on uniform effective temperature and abundance scales. Error bars are 1 σ errors estimated as described in the text. (*a*) Entire sample. (*b*) Subsample with [Fe/H] > −2.25. *Solid line*: planar fit to entire sample in $T_{\rm eff}$ and [Fe/H], evaluated at the median metallicity for this subgroup ([Fe/H] = −1.8). (*c*) Subsample with −2.75 < [Fe/H] < −2.25. *Solid line*: planar fit evaluated at [Fe/H] = −2.6. *Dotted line*: 18 Gyr Li isochrone at [Fe/H] = −2.3 with diffusion, computed for initial A(Li) = 2.40 by Chaboyer & Demarque. *Dashed lines*: combined effects of diffusion and rotation computed by Chaboyer & Demarque, for initial rotation velocities 10 km s^{-1} (*upper*) and 30 km s^{-1} (*lower*), at [Fe/H] = −2.3, 14 Gyr, for initial A(Li) = 3.03. (*d*) Subsample with [Fe/H] < −2.75. *Solid line*: planar fit evaluated at [Fe/H] = −3.1. *Dotted line*: 18 Gyr Li isochrone at [Fe/H] = −3.3 with diffusion, computed for initial A(Li) = 2.45 by Chaboyer & Demarque (1994). *Dashed lines*: combined effects of diffusion and rotation computed by Chaboyer & Demarque, for initial rotation velocities 10 km s^{-1} (*upper*) and 30 km s^{-1} (*lower*), at [Fe/H] = −3.3, 14 Gyr, for initial A(Li) = 2.87.

the data, without responding inordinately to the presence of modest and extreme (high-leverage) outliers. Such an approach seems appropriate for data of this sort, as unrecognized systematics in just a few stars should not be permitted to dominate the derived results.

4.1.1. *Weighted Least-Squares Analysis*

We begin by discussing the morphology of the data rather than its astrophysical interpretation; the latter follows below. A multiple regression fit (Bevington 1969, Chapter 9), weighted according to the formal error in A(Li), and linear in both $T_{\rm eff}$ and [Fe/H] yields

$$A(\mathrm{Li}) = -0.39(\pm 0.14) + 0.043(\pm 0.002)T_{\rm eff}/100 + 0.044(\pm 0.008)[\mathrm{Fe/H}] ,$$

where the parenthetic quantities are 1 σ errors in the coefficients. The metallicity coefficient is smaller than that obtained by Thorburn (viz., 0.13 ± 0.03 dex per dex). This may reflect the finding of Norris et al. that the metallicity dependence of Li diminishes at metallicities above [Fe/H] = −2.0 (where Thorburn's sample was minimal), but it is also affected by the different choice of stellar atmospheres (see below).

We also computed separate regressions of the form A(Li) = A0 + A1 × $T_{\rm eff}$/100 for each metallicity bin of Figures 3*b*–3*d*. Naturally this produced a slightly different fit to that above, but nevertheless the $T_{\rm eff}$ coefficients were highly significant, 6–11 times the formal errors, for each bin, as expected for such clear trends. In the following section we compute robust regressions, and in Figures 3*b*–3*d* we show the favored fit, given in the abstract, evaluated at the median metallicity of each bin.[7] A change we could have made to improve the fit would be to include a cross term in $T_{\rm eff}$[Fe/H], which would permit a lower $T_{\rm eff}$ slope at the lowest metallicities. We refrain from this because of the risk of overinterpreting the data.

Our claim of the persistence of trends with [Fe/H] and $T_{\rm eff}$ is at odds with the analysis by Molaro, Primas, & Bonifacio (1995), which claims that the plateau is uniform and flat. Molaro et al. adopt a new $T_{\rm eff}$ scale based on Balmer lines, hotter than the photometric scales by typically 125 ± 120 K. The main effect of the temperature change is to shift the Li abundances en masse, by 0.1 ± 0.1 dex, rather than to redistribute the data in a major fashion. They performed separate regressions on $T_{\rm eff}$ and on [Fe/H], finding no significant trends. However, as Norris et al. (1994) endeavored to show, the trends become clear once the parameters are treated together, either by dividing the sample into smaller metallicity ranges or alternatively by doing a multiple regression on both quantities simultaneously (Thorburn 1994). If the Molaro et al. data set is restricted to $T_{\rm eff}$ > 5500 K, [Fe/H] ≤ −1.2, and subgiants are excluded (treating HD 140283 and HD 166913 as such), a planar regression yields the fit

$$A(\mathrm{Li}) = 0.60(\pm 0.50) + 0.025(\pm 0.009)T_{\rm eff}/100 - 0.02(\pm 0.32)[\mathrm{Fe/H}] .$$

A trend with [Fe/H] is not identified, perhaps owing to the paucity of stars with [Fe/H] < −3.0 in their sample, but the $T_{\rm eff}$ trend is recovered, comparable with that in our study. Eventual application of Balmer temperatures to the entire Li dwarf sample will be a valuable undertaking to reduce some of the uncertainties associated with photometric calibrations and reddenings.

4.1.2. *A Reweighted Least-Squares Analysis (Based on the Least Median of Squares)*

There are a number of concerns associated with using the standard weighted least-squares (hereafter WLS) technique for the regression of A(Li) on $T_{\rm eff}$ and [Fe/H]. The most serious worry is that relatively few points with claimed small statistical errors, but located in crucial high-leverage positions within the data, may be dominating the resultant determination of the coefficients and hence the trends we are investigating. In this section we explore alternative approaches as a means of evaluating how much the choice of regression technique is indeed

[7] We note that the "high" Li abundances for BD +72°94 and G21−22 do not drive the regressions, as their large formal errors produce small weights in the weighted least-squares analysis, and the robust analysis of § 4.1.2 is resistant to isolated extreme points.

influencing the results. We also consider how variations of the subsample selection with temperature (and exclusion of the seven additional possible subgiants) may affect the calculation. We choose to investigate six data batches:

Sample A.—Our original homogenized data with [Fe/H] ≤ -1.2, $T_{\rm eff} > 5500$ K (RBDT scale) ($N = 94$).

Sample A.*—Our original homogenized data with the "possible" subgiants removed, with [Fe/H] ≤ -1.2, $T_{\rm eff} > 5500$ K (RBDT scale) ($N = 87$).

Sample B.—Our homogenized data with [Fe/H] ≤ -1.4, $T_{\rm eff} > 5700$ K (RBDT scale) ($N = 85$).

Sample B.*—Our homogenized data with the "possible" subgiants removed, with [Fe/H] ≤ -1.4, $T_{\rm eff} > 5700$ K (RBDT scale) ($N = 80$).

Sample C.—The original Molaro et al. data with [Fe/H] ≤ -1.4, $T_{\rm eff} > 5700$ K (Molaro scale) ($N = 24$).

Sample D.—The Molaro et al. data *minus* the two stars we classify as subgiants, with [Fe/H] ≤ -1.4, $T_{\rm eff} > 5700$ K (Molaro scale) ($N = 22$).

Samples B and B* are defined so that we are well away (on any sensible temperature scale) from the region of the cool side of the Li plateau, where depletion arising from stellar processes is expected to become severe. We have also restricted sample B to stars with metallicities which match the cutoff employed by Molaro et al., to see what, if any, effect this might have on the resulting regressions.

For each of these four subsamples, we carry out regressions according to the following models:

Model 1.—$A(\rm Li) = A0 + A1(T_{\rm eff})$.
Model 2.—$A(\rm Li) = A0 + A1[Fe/H]$.
Model 3.—$A(\rm Li) = A0 + A1(T_{\rm eff}) + A2[Fe/H]$.

Each of the regressions is obtained twice, first with a standard unweighted least-squares (hereafter LS) approach (which differs from that of the previous section because statistical weights are not considered), and then with the reweighted least-squares technique based on the least median of squares (hereafter RLS/LMS) approach of Rousseeuw & Leroy (1987). This technique implements an objective identification of outliers based on deviations from a resistant regression fit (using LMS) obtained from multiple resamples of the original data. Once identified, these outliers are removed from the sample and a standard unweighted least-squares technique is applied to the surviving data.

The results of our regressions are summarized in Table 6. Column (1) lists the sample under investigation. Column (2) is the number of stars contained in the sample. Column (3) iden-

TABLE 6

RESULTS OF THE REGRESSION FITS OF A(Li) ON $T_{\rm eff}$ AND [Fe/H]

Sample (1)	N (2)	Model (3)	Technique (4)	A0 (Constant)[a] (5)	A1 ($T_{\rm eff}$/100 K)[a] (6)	A2 ([Fe/H])[a] (7)	Outliers (8)	R^{2} [b] (9)
A	94	1	LS	0.189 (0.351, 0.592)	0.0316 (0.0058, 0.000)	...	...	0.242 (0.000)
	90	1	RLS/LMS	−0.124 (0.329, 0.709)	0.0367 (0.0055, 0.000)	...	4	0.340 (0.000)
	94	2	LS	2.201 (0.056, 0.000)	...	0.043 (0.022, 0.055)	...	0.039 (0.055)
	91	2	RLS/LMS	2.260 (0.054, 0.000)	...	0.066 (0.021, 0.003)	3	0.096 (0.003)
	94	3	LS	−0.216 (0.321, 0.502)	0.0422 (0.0056, 0.000)	0.097 (0.019, 0.000)	...	0.413 (0.000)
	91	3	RLS/LMS	−0.090 (0.302, 0.765)	0.0408 (0.0052, 0.000)	0.111 (0.018, 0.000)	3	0.464 (0.000)
A*	87	1	LS	−0.023 (0.349, 0.948)	0.0350 (0.0058, 0.000)	...	...	0.301 (0.000)
	84	1	RLS/LMS	−0.243 (0.325, 0.455)	0.0387 (0.0054, 0.000)	...	3	0.388 (0.000)
	87	2	LS	2.181 (0.061, 0.000)	...	0.036 (0.024, 0.135)	...	0.026 (0.135)
	85	2	RLS/LMS	2.141 (0.060, 0.000)	...	0.020 (0.023, 0.384)	2	0.009 (0.384)
	87	3	LS	−0.359 (0.320, 0.265)	0.0443 (0.0055, 0.000)	0.092 (0.019, 0.000)	...	0.448 (0.000)
	84	3	RLS/LMS	−0.527 (0.296, 0.079)	0.0468 (0.0051, 0.000)	0.084 (0.018, 0.000)	3	0.519 (0.000)
B	85	1	LS	0.478 (0.402, 0.238)	0.0268 (0.0066, 0.002)	...	...	0.164 (0.000)
	81	1	RLS/LMS	0.459 (0.359, 0.205)	0.0273 (0.0059, 0.000)	...	4	0.213 (0.000)
	85	2	LS	2.204 (0.060, 0.000)	...	0.040 (0.023, 0.092)	...	0.034 (0.092)
	83	2	RLS/LMS	2.240 (0.057, 0.000)	...	0.054 (0.022, 0.017)	2	0.068 (0.017)
	85	3	LS	0.020 (0.384, 0.959)	0.0381 (0.0066, 0.000)	0.091 (0.022, 0.000)	...	0.311 (0.000)
	79	3	RLS/LMS	0.292 (0.323, 0.368)	0.0334 (0.0056, 0.000)	0.082 (0.019, 0.000)	6	0.351 (0.000)
B*	80	1	LS	0.275 (0.414, 0.509)	0.0301 (0.0068, 0.000)	...	...	0.200 (0.000)
	76	1	RLS/LMS	0.275 (0.366, 0.456)	0.0303 (0.0060, 0.000)	...	4	0.254 (0.000)
	80	2	LS	2.203 (0.062, 0.000)	...	0.040 (0.024, 0.102)	...	0.034 (0.102)
	78	2	RLS/LMS	2.168 (0.059, 0.000)	...	0.029 (0.023, 0.202)	2	0.021 (0.202)
	80	3	LS	−0.184 (0.389, 0.637)	0.0415 (0.0067, 0.000)	0.092 (0.021, 0.000)	...	0.355 (0.000)
	75	3	RLS/LMS	0.009 (0.331, 0.979)	0.0384 (0.0057, 0.000)	0.091 (0.018, 0.000)	5	0.424 (0.000)
C	24	1	LS	1.434 (0.644, 0.036)	0.0126 (0.0105, 0.244)	...	...	0.061 (0.243)
	23	1	RLS/LMS	1.070 (0.606, 0.092)	0.0187 (0.0099, 0.073)	...	1	0.145 (0.073)
	24	2	LS	2.204 (0.102, 0.000)	...	0.000 (0.042, 0.996)	...	0.000 (0.996)
	22	2	RLS/LMS	2.194 (0.090, 0.000)	...	−0.011 (0.037, 0.765)	2	0.005 (0.765)
	24	3	LS	1.269 (0.699, 0.084)	0.0165 (0.0122, 0.191)	0.031 (0.047, 0.519)	...	0.080 (0.417)
	24	3	RLS/LMS	1.269 (0.699, 0.084)	0.0165 (0.0122, 0.191)	0.031 (0.047, 0.519)	0	0.080 (0.417)
D	22	1	LS	1.077 (0.679, 0.129)	0.0183 (0.0111, 0.114)	...	...	0.120 (0.114)
	18	1	RLS/LMS	−0.409 (0.534, 0.454)	0.0428 (0.0087, 0.000)	...	4	0.601 (0.000)
	22	2	LS	2.180 (0.108, 0.000)	...	−0.007 (0.044, 0.875)	...	0.001 (0.875)
	22	2	RLS/LMS	2.180 (0.108, 0.000)	...	−0.007 (0.044, 0.875)	0	0.001 (0.875)
	22	3	LS	0.837 (0.748, 0.277)	0.0237 (0.0131, 0.000)	0.039 (0.049, 0.434)	...	0.149 (0.217)
	20	3	RLS/LMS	−0.067 (0.655, 0.919)	0.0387 (0.0114, 0.003)	0.046 (0.040, 0.256)	2	0.415 (0.011)

NOTE.—Recall that samples A* and B* have had the "possible" subgiants removed.
[a] Numbers in parentheses are the error of the coefficient and its associated p-value.
[b] Number in parentheses is associated p-value.

tifies the regression model. Column (4) lists the technique employed for the regression. Column (5) is the constant term in the regression, along with the error in the coefficient, and its associated p-value. The p-value is the (two-sided) probability that a Student-distributed random variable with the appropriate degrees of freedom (i.e., number of points diminished by the number of fitting parameters) becomes larger in absolute value than expected for the null hypothesis that the coefficient on this parameter is equal to zero, and it can be taken as an indication of the significance of the dependence of A(Li) on this parameter. Column (6) is the coefficient of $T_{\rm eff}$ (scaled by 100 K), its estimated 1 σ error, and its associated p-value. Column (7) is the coefficient of [Fe/H], its 1 σ error, and its associated p-value. Column (8) lists the number of outliers which are identified by the LMS procedure. Column (9) is the coefficient of determination, R^2 (the square of the Pearson correlation coefficient), which provides an indication of the amount of variation of A(Li) which can be accounted for by the regression model under consideration (the coefficient of determination always lies in the range $0 \leq R^2 \leq 1$). Also listed in this column is the associated p-value, which provides a measure of significance of the entire vector of regression coefficients (i.e., a test of the hypothesis that all [nonconstant] predictor variables have coefficients equal to zero).

Inspection of Table 6 reveals a number of interesting results. We discuss the samples on a case by case basis.

Sample A.—The LS regression on $T_{\rm eff}$ obtains a smaller (but still highly significant) slope than derived above with the WLS technique. However, R^2 indicates that only 24% of the variation in A(Li) is accounted for by the dependence on $T_{\rm eff}$. The LMS pass through the data reveals four suspected outliers. When these stars are removed, and an LS regression is applied to the surviving data, the slope on $T_{\rm eff}$ increases to a value in concert with that obtained above. At the same time, the R^2 value increases somewhat (to 34%).

The LS regression reveals only a marginally significant dependence on [Fe/H] when it is used as the sole independent variable. The RLS/LMS regression (three outliers removed) indicates no significant dependence on [Fe/H] when it is used as the sole independent variable.

When the multiple regression model is employed, both the LS and RLS/LMS techniques indicate that significant dependence on $T_{\rm eff}$ and [Fe/H] exist in this sample. Note that the coefficient on $T_{\rm eff}$ is similar to that obtained with the WLS technique, but the coefficient on [Fe/H] increases relative to our previous determination, to on the order of 0.1 dex per dex in [Fe/H], similar to that derived by Thorburn (1994). In the RLS/LMS analysis (three outliers removed), the coefficient of determination, R^2, indicates that 46% of the variation of A(Li) is now captured by the multiple regression fit.

One always has to be concerned with the presence of multicolinearity among the predictor variables, in this case $T_{\rm eff}$ and [Fe/H]. Both the Pearson correlation coefficient and the Spearman rank correlation coefficient indicate that these variables exhibit modest, but not strong, colinearity, on the order of 0.4. A high value of this coefficient would indicate that either variable could be used to predict the other, calling into question the need to include both predictors in the regression model and possibly perturbing the interpretation. A plot of [Fe/H] as a function of $T_{\rm eff}$ is shown in Figure 4. It would clearly be of interest to obtain additional observations of A(Li) for the regions of this diagram which are not well populated at

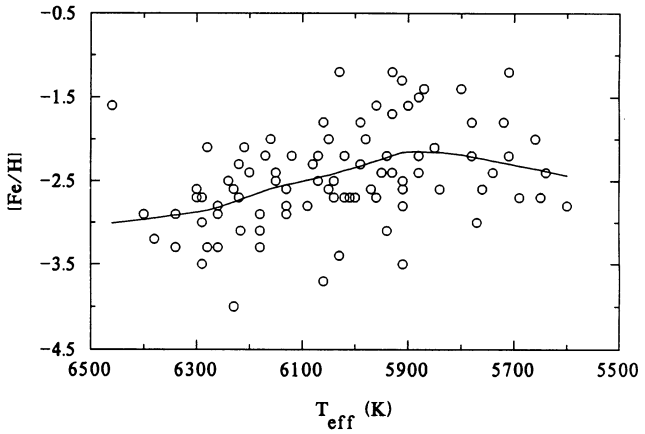

FIG. 4.—Distribution of [Fe/H] and $T_{\rm eff}$ for the stars in sample A. The solid line (obtained from a locally weighted resistant regression) indicates the existence of a modest, but detectable, correlation between these variables.

present; i.e., additional stars with $-2.5 \leq$ [Fe/H] ≤ -1.2 and $T_{\rm eff} > 6000$ K, and stars with [Fe/H] ≤ -3.0 and 5600 K $\leq T_{\rm eff} \leq 6000$ K. Metal-deficient stars on the cool end of the diagram are a challenge to identify and study, but they should be given high priority in future investigations.

The necessity of a dependence on [Fe/H], in addition to that on $T_{\rm eff}$, may also be seen from inspection of Figure 5, where we plot the distribution of residuals in A(Li) obtained from the RLS/LMS technique as a function of [Fe/H] when $T_{\rm eff}$ is the lone predictor. Note that including the outliers identified by the LMS pass through the data would suggest an even larger effect. The radii of the circles in Figure 6 show the RLS/LMS residuals obtained in A(Li) over the [Fe/H], $T_{\rm eff}$ plane when both variables are included. Note that the distribution of residuals for the multiple correlation model is rather good, with no preponderance of positive or negative residuals in any given region of the map. This is also indicated by Figure 7, which is a histogram of the residuals in A(Li) for the multiple correlation model. The mean of the residuals is 0.000 dex, with a dispersion of 0.089 dex.

Sample A.*—As is seen in Table 6, removal of the seven "possible" subgiants from sample A does not significantly

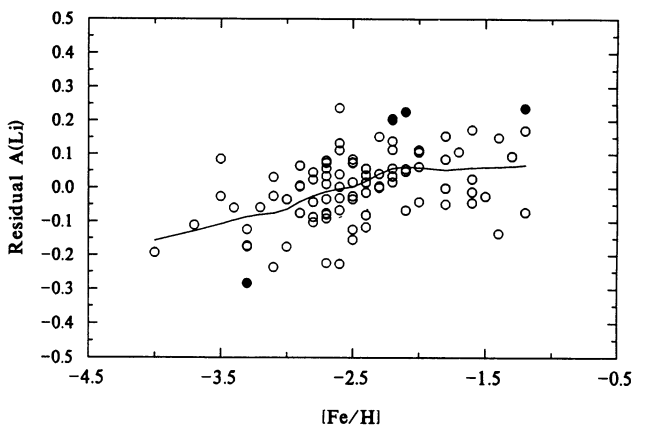

FIG. 5.—Distribution of residuals of A(Li) [in the sense predicted A(Li) minus observed A(Li)] as a function of [Fe/H] obtained for the sample A stars when only $T_{\rm eff}$ is used as a predictor variable in the RLS/LMS procedure. Suspected outliers identified by the LMS procedure are indicated with filled circles. A clear trend with [Fe/H] is indicated by the solid line (obtained from a locally weighted resistant regression).

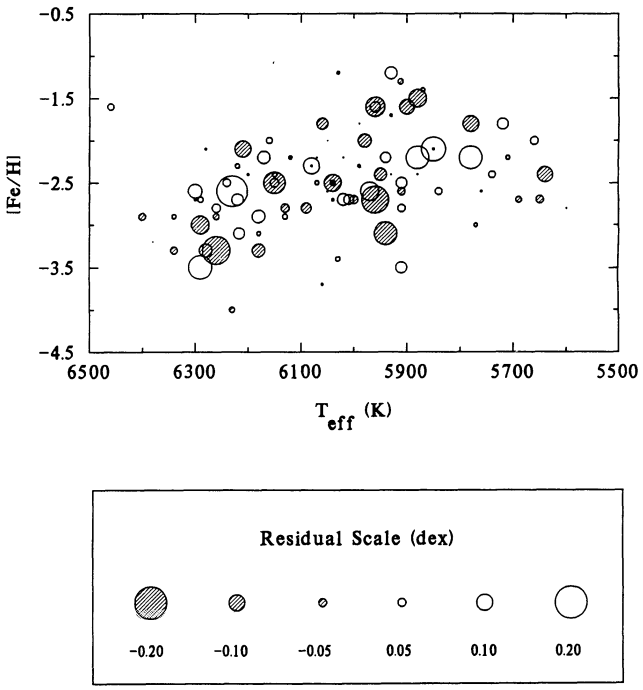

FIG. 6.—Map of residuals of A(Li) obtained for the sample A stars in the [Fe/H], $T_{\rm eff}$ plane. The radius of each circle is directly proportional to the size of the residual; a scale is shown below. The open circles represent positive residuals, while the cross-hatched circles indicate negative residuals. Note that outliers (listed in the column labeled "A3" of Table 7) are not shown.

alter the results of our regressions when $T_{\rm eff}$ is used as the lone predictor, but when [Fe/H] serves as the lone predictor the slope on [Fe/H] decreases (to the level that it is no longer significant). The results of the multiple regression model are consistent with those obtained for sample A.

Sample B.—When our sample is restricted to exclude the nine lowest temperature dwarfs and/or higher metallicity stars, inspection of Table 6 indicates that rather similar results are obtained as for the regressions obtained on sample A, suggesting that our results are not crucially dependent on the low-temperature or upper metallicity cutoffs.

Sample B.*—Removal of the "possible" subgiants from sample B does not significantly alter the results of our regressions, as indicated in Table 6.

Sample C.—This sample is defined identically to that examined by Molaro et al. (1995) with a standard WLS technique.

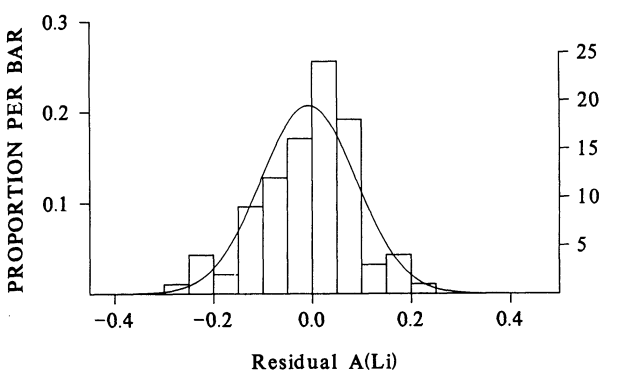

FIG. 7.—Distribution of residuals of A(Li) obtained for the sample A stars in the [Fe/H], $T_{\rm eff}$ plane. The solid line is the best-fit Gaussian.

The results of our LS and RLS/LMS analyses are qualitatively similar to those obtained by Molaro et al. No significant dependence is found on A(Li) when regressed against $T_{\rm eff}$ or [Fe/H] considered as lone predictors, or when considered together in the multiple regression model. Thus, the differences between our claims and those of Molaro et al. are most likely attributable to the different stars included in the sample.

Sample D.—When the two suspected subgiants excluded from our sample (HD 140283 and HD 166913) are removed from the Molaro et al. data, the results change as follows.

The LS regression of A(Li) on $T_{\rm eff}$ shows only a slight increase over that obtained from sample C (but still not significant). However, the LMS pass through this reduced data set (after removal of four outliers) indicates that the coefficient on $T_{\rm eff}$ increases to a value similar to that obtained above for our data set and becomes highly significant. The R^2 coefficient of determination reaches 60%, the highest found in any of our analyses. The regression on [Fe/H] remains insignificant when it is considered as the lone predictor.

When both $T_{\rm eff}$ and [Fe/H] are considered in the multiple regression model, a strong dependence on $T_{\rm eff}$ is again recovered, similar to the slopes obtained for our data set, while the slope on [Fe/H] remains insignificant. The fact that such different results on the correlation with $T_{\rm eff}$ are obtained when only two stars (the subgiants) are removed is the key to our different conclusions. As discussed in § 3.2, we exclude subgiants on the grounds that they had different main-sequence temperatures and evolutionary histories to the plateau *dwarfs* still on the main sequence.

Table 7 lists the outliers identified by the LMS technique for the indicated combination of sample and regression model. The final column lists the number of independent measurements of A(Li) for the star under consideration. It is important to obtain repeat, high-quality reobservations of these stars in order to ascertain whether or not the Li abundances for these stars are truly discrepant, or whether they appear on our list of suspected outliers as a result of errors of measurement. The star BD +42°3607 and the star G64−37 appear several times as outliers in the Molaro et al. sample.

4.1.3. *Interpretations*

To what extent are these trends real, reflecting astrophysical processes, and to what extent are they artifacts of the analysis? As noted in § 3.3, the abundance one derives depends not only upon an adopted effective temperature but also upon the model structure. Figure 2 shows that the Bell and Kurucz models give abundances that differ not only in zero point but also in scale. Two stars at 5600 K and 6300 K, for which the Bell models give identical abundances, would have according to the Kurucz models abundances which differ by 0.05 dex, the cooler star being more Li rich. Changing from the Bell models to the Kurucz models would result in a reduction of the $T_{\rm eff}$ slope from 0.038 dex per 100 K to 0.031 dex per 100 K (obtained from the WLS regression), diminishing but not eliminating a significant slope.

The models also differ in their metallicity dependence. Again as illustrated in Figure 2, the Kurucz models show greater differences between models at [Fe/H] = −1 and −2 than the Bell models show, with the effect that changing to the Kurucz models would increase the derived dependence on metallicity, but by at most 0.02 dex per dex. It is difficult to argue that metallicity-dependent errors in the temperature calibration have produced the observed trends because colors become less

TABLE 7

OUTLIERS REJECTED BY RLS/LMS TECHNIQUE

STAR	SAMPLE AND MODEL												OBSERVATIONS
	A1	A2	A3	B1	B2	B3	C1	C2	C3	D1	D2	D3	
BD +03°740	–	–	–	–	–	–	–	–	–	Y	–	–	6
BD +09°2190	–	–	–	–	–	–	–	–	–	Y	–	–	2
BD +42°3607	Y	–	–	–	–	–	–	–	–	Y	–	Y	1
CD −33°1173	Y	–	–	Y	–	Y	xx	xx	xx	xx	xx	xx	3
LP 553−62	–	–	Y	Y	–	Y	xx	xx	xx	xx	xx	xx	1
CS 22186−017	–	–	–	Y	–	Y	xx	xx	xx	xx	xx	xx	1
G21−22	–	Y	–	–	Y	Y	xx	xx	xx	xx	xx	xx	1
G64−37	–	–	–	–	–	–	Y	Y	–	Y	–	Y	3
G169−4	–	–	–	Y	–	Y	xx	xx	xx	xx	xx	xx	1
HD 3567[a]	Y	–	–	–	–	–	–	–	–	–	–	–	1
HD 24289[a]	Y	–	–	–	–	–	xx	xx	xx	xx	xx	xx	2
HD 116064	–	–	–	–	–	–	–	Y	–	–	–	–	1
HD 193901	–	Y	Y	–	–	–	–	–	–	–	–	–	1
HD 201891	–	Y	Y	–	Y	Y	–	–	–	–	–	–	4

NOTE.—Y = outlier rejected by RLS/LMS technique. – = not rejected as outlier by RLS/LMS analysis. xx = not in Molaro et al. sample.

[a] Flagged in text as possible subgiant.

sensitive to metallicity for more metal-deficient stars, but the metallicity trend in Li abundances does *not* diminish in the lowest metallicity stars. In Figures 3*b*–3*d* we plot lines giving the fit for the full sample (A) analyzed with the RLS/LMS technique, evaluated at the median metallicity of each sample.

Because the $T_{\rm eff}$ trend slope is of order 0.040 dex per 100 K, and the sensitivity of A(Li) to $T_{\rm eff}$ in a given star is 0.08 dex per 100 K, attempts to remove the slope by changing the effective temperature scale would have to compress the effective temperature range currently ascribed to the plateau by a factor of 2, but there appears to be no reason to justify a temperature scale change of this magnitude. We conclude that either the current models are radically inappropriate for Li, perhaps as Kurucz (1995) has discussed, or the $T_{\rm eff}$ trend is real; minor revisions of the effective temperature scale or model structure appear unlikely to eliminate the trends.

The [Fe/H] trend is statistically significant according to tests of the sample, but in contrast to the situation for the $T_{\rm eff}$ trend, it is relatively easy to envisage a systematic revision to stellar atmosphere models that *might* eliminate it. For example, we discussed in § 3.3 that A(Li) changes of 0.1–0.2 dex could be obtained by switching to Kurucz's newer models in which convection is handled differently. If the effects of convection depend on metallicity (which is a reasonable expectation), it is conceivable that future revisions of systematics could modify this trend, and we cannot exclude its eventual elimination by such changes.

4.1.4. *Discussion of Trends*

To summarize, the full data sample when analyzed using a homogeneous effective temperature scale retains stronger $T_{\rm eff}$ and [Fe/H] dependences than can be readily accounted for by differences between current atmospheric models or by non-LTE effects. The astrophysical implications in the case in which the trends are real have been discussed previously by Thorburn (1994) and by Norris et al. (1994). These consider Li depletion in plateau stars as a function of temperature and/or metallicity, and possible Galactic enrichment of Li contributing to the observed metallicity dependence. Models of Li, Be, and B production by spallation that take into account characteristics of the halo, in particular exclusion of some gas from star formation (Ryan et al. 1992; Prantzos, Casse, & Vangioni-Flam 1993), can provide good agreement with observed halo Be and B abundances but may produce considerably more Li than is observed at the Spite plateau. However, as discussed by Deliyannis et al. (1995), this oversupply of Li is only a problem if one maintains that the plateau corresponds to the primordial abundance, a tenet which the observations now challenge, showing significant temperature and metallicity trends and star-to-star differences in the plateau (to be discussed in § 4.3).[8] Once the possibilities of post–big bang synthesis of Li appearing in halo stars and nonnegligible processing of Li by these stars are admitted, as seems required by the data, the problem of determining the primordial Li abundances becomes less well constrained. A better understanding of stellar processing of Li and of cosmic-ray acceleration and propagation will aid clarification of these issues.

On the alternative possibility that the models are *seriously* inapplicable, Kurucz (1995) has challenged the applicability of one-dimensional models to the analysis of Li and even possibly Fe (among other elements), since these models ignore the effects of convection on the three-dimensional temperature distribution and ionization. If his concerns are fully justified, then many results of stellar abundance analyses will have to be reconsidered, not just those for Li. However, until genuine three-dimensional computations of Li line propagation are undertaken, we proceed with an analysis based on the one-dimensional models.

4.2. Li *Diffusion in Halo Dwarfs*

Diffusion in halo stars is potentially interesting because of (*a*) implications for inferring the primordial Li abundance and (*b*) implications for reducing globular cluster age estimates. As discussed in § 2, models incorporating diffusion predict a downturn in Li abundances near the halo main-sequence turnoff. In Figures 3*c*–3*d* we show the recent diffusive isochrones of Chaboyer & Demarque (1994, their Fig. 6) as dotted lines. These were computed for higher initial Li abundances

[8] In fact, the overproduction of Li relative to Be and B by the $\alpha + \alpha$ reaction itself depends on uncertain aspects of cosmic-ray acceleration and spallation in a metal-poor interstellar medium, e.g., Fields, Olive, & Schramm (1994).

than we would infer, so they could be shifted downward by some amount. Of importance in our comparison is their shape, in particular the poor agreement to the trend with $T_{\rm eff}$. No downturn is evident for the hot stars, as reported in our earlier statements (Deliyannis et al. 1992; Ryan 1993) and echoed for the Thorburn sample by Thorburn (1994) and by Chaboyer & Demarque (1994). We conclude that the signature expected of uninhibited diffusion based on current models is far from obvious in these stars.

For one star in the lowest metallicity group (Fig. 3*d*), only an upper limit on A(Li) is available. Further observations are required to clarify its nature, such as whether it belongs to the class of extremely Li depleted dwarfs, or whether some other mechanism is responsible for its depressed Li abundance. The current paucity of cool, extremely metal-poor dwarfs hinders further investigation of this metallicity class.

Chaboyer & Demarque also discussed combined rotation + diffusion models. In Figures 3*c*–3*d* we show their combined isochrones as dashed lines. Although at [Fe/H] = −2.3 the combined isochrones appear attractive, being less curved than the pure diffusive ones and allowing for a range of Li abundances, at [Fe/H] = −3.3 the two types have indistinguishable shapes and are unacceptable because of the lower abundances predicted for hotter stars. We conclude that neither the pure diffusive nor the combined diffusive + rotating models currently provide an acceptable fit to the data.

Because the depth of the surface convection zone near the turnoff (and hence the degree of diffusion predicted there) is model dependent, the question of whether diffusion acts uninhibited or whether some mechanism (mixing?) reduces the efficiency of diffusion must remain open. Nevertheless, from the excessive curvature seen in the diffusion isochrones relative to the observations, we conclude that uninhibited diffusion is unlikely to result in an initial Li abundance more than of order 0.1 dex higher than that inferred from models that ignore diffusion. (If a mechanism other than diffusion, such as nonconvective mixing, is also taking place, then a significantly higher initial abundance is possible.) By contrast, possible reduction of globular cluster age estimates by diffusion is less well constrained because even a little He diffusion can reduce inferred ages. Furthermore, if mixing is sufficient to transport material to depths at which Li is destroyed, then Li will not trace He diffusion, although such mixing might homogenize the He profile and reduce or even negate inferred age reductions; the details of such possibilities have yet to be computed.

In the previous section we found that the $T_{\rm eff}$ scale would have to be compressed by an unrealistic amount (factor of 2) to eliminate the observed slope of Li with $T_{\rm eff}$. However, other changes in the $T_{\rm eff}$ scale can have implications for diffusion. If the scale is compressed more for turnoff stars than further down the main sequence, as with the scale of King (1993) (see Deliyannis et al. 1995), then Li abundances of turnoff stars will be reduced more than for cooler stars, admitting more curvature to the plateau and possibly a renewed signature of diffusion. Improved understanding of $T_{\rm eff}$ scales is clearly desirable to better constrain the effects of diffusion.

4.3. *Dispersion in the Spite Plateau*

Several authors have investigated the existence and astrophysical implications of a possible spread in the Li abundances of plateau stars, over and above that explainable in terms of temperature trends (Deliyannis, Pinsonneault, & Duncan 1993; Thorburn 1994). We begin by asking whether the spread in measurements of the Li equivalent width for each star with multiple observations is consistent with the formal errors. Second, we briefly discuss evidence concerning an intrinsic spread in the plateau in excess of reasonable errors, but we defer a major discussion to a separate paper.

4.3.1. *Errors in the* Li *Equivalent Width Observations*

We assume in the following that real equivalent width variations do not occur for Li in these stars. Given the lack of variation found by Boesgaard (1991) for Li in chromospherically active stars, and the low expectation of finding heavily spotted stars of this age and temperature which might exhibit changes, this assumption seems reasonable.

The significance of the spread in Li abundances depends on how realistic the error estimates are. Table 2 presents multiple (two to five) Li equivalent width measurements for 37 stars. For each of these stars we compute a reduced χ^2 statistic which measures the spread of the measurements about their σ-weighted mean (§ 3), and subsequently we obtain the probability that a larger reduced χ^2 value would arise randomly. In a sample of 37 stars with repeat observations affected by correctly estimated, purely Gaussian errors, one star would be expected to have a χ^2 probability less than 100/37 = 2.7%. The actual probability distribution is reasonably uniform over most of the range, confirming that for the great majority of cases, the scatter between multiple observations is consistent with the stated errors, which is to say that the latter are reasonable estimates of the true errors. Moreover, this indicates a regularly attained precision of a few mÅ. However, whereas we expect only one star to exhibit a probability below 2.7%, we in fact find five, four more than expected, which we flag with exclamation points in Tables 2 and 3. If we take the conservative approach of saying that just one measurement is particularly poor for each star, it follows that there are four "bad" measurements out of the 109 made for these 37 stars.

While our analysis does not pertain to the Thorburn or the Deliyannis et al. studies explicitly, it demonstrates that errors estimated from S/N and resolution considerations alone are not always adequate for assessing the reliability of a measurement, since other errors, often difficult to identify, can contribute and produce rare but large errors which are not adequately gauged by standard error analyses. Sources of such errors might include poor continuum placement, low-intensity cosmic-ray strikes, scattered light in spectrographs, electronic variations during CCD readout, etc. Deliyannis et al. set a lower limit of 2.0 mÅ on $\sigma(W)$ in their analysis to help contain the effects of low-level errors. Application of such a limit in the current work would reduce the number of stars flagged as having discrepant measurements from five to two (LP 815-43 and BD −13°3442), though it might also underrate the high-precision data available for some stars, for example, HD 84937, for which the five measurements with $\sigma(W)$ = 1.0 are all in good agreement. The small number of stars common to several databases prevented us (§ 3.2) from quantifying systematic errors which might exist between studies, except in one case for which we determined a 3 mÅ offset. Other less obvious non-Gaussian errors in equivalent widths, perhaps concealed by larger random errors and/or the lack of sufficient comparison observations, can affect both the combination of multiple observations of a single star and the combination of many stars to investigate a spread about the plateau. Unless multiple observations of high accuracy are available for stars used in

dispersion analyses, there is a nonnegligible risk that unrecognized large errors may be present which will contribute to greater scatter than is expected. Since it is scatter in excess of expected errors which is the diagnostic for any investigation of intrinsic dispersion, and since dispersion will usually be increased rather than decreased by additional error sources, it would be valuable to obtain multiple (perhaps three) observations of program stars at high precision to show that the random error estimate for each star is reasonable. Samples might also be chosen over narrow color, metallicity, and evolutionary ranges to minimize the effects of other differences between the stars. Errors in temperature determinations and reddening will also have significant non-Gaussian components which must be treated cautiously when considering combining diverse samples of stars to investigate an intrinsic spread.

4.3.2. *Intrinsic Scatter in the Plateau?*

Descriptions of Li data could range between the extremes in which (1) the plateau is discussed as if there were just one Li value in all plateau stars with experimental errors accounting fully for the observed scatter, to the other extreme (2) in which most if not all stars have different values of Li owing to influences other than uniform big bang nucleosynthesis. We find the first extreme very difficult to embrace, given examples of stars with very different Li abundances but seemingly very reliable data, which we discuss in subsequent paragraphs. We defer discussion of whether or not a spread is a *global* characteristic of halo dwarfs to a forthcoming paper, where we address how far toward the other extreme the true situation may be. In this section we restrict our discussion to those stars for which multiple observations have already been obtained, and we inspect the data for significant differences between stars.

The Li abundances of G64 − 12 and G64 − 37 are in remarkable contrast to one another (Deliyannis et al. 1992). To that comparison we add the star CD −33°1173. These stars have five, three, and three equivalent width measurements, respectively, with good agreement between the multiple measurements. The first two are in a similar direction in the Galaxy (Lowell field 64), and all three have low reddening, similar colors, and inferred $T_{\rm eff}$ values, are close to the turnoff, and have similar very low metallicities[9] $-3.5 \leq$ [Fe/H] ≤ -3.0, yet the abundances given in Table 3 are A(Li) = 2.29 ± 0.05, 2.01 ± 0.04, and 1.89 ± 0.06, respectively. It seems unlikely that errors of measurement or analysis can be invoked to eliminate the differences between these three, and they may offer irrefutable evidence of a Li abundance spread for at least *some* of the stars on the plateau. The cause of the difference is not clear, though possible explanations such as the effects of different rotational histories are discussed in the literature (Deliyannis et al. 1993; Thorburn 1994), and we may speculate about the effects of unrecognized binarity, subtly different evolutionary and/or magnetic histories, or the possibility that the mechanism inhibiting diffusion in most plateau binaries is modified in some stars such as G64 − 37. A detailed comparison of these otherwise similar stars could be a rewarding project.

5. CONCLUSIONS

We present new Li data on seven halo turnoff stars to test for evidence of diffusion acting in their outer layers, based on spectra obtained with the coudé spectrograph on the Canada-France-Hawaii Telescope. These data are combined with equivalent widths obtained from the literature, and new effective temperatures and Li abundances are computed for the entire set on uniform temperature and abundance scales.

We find that the Li abundance trends with effective temperature and with [Fe/H] discussed by Thorburn (1994) and Norris et al. (1994) are present in the homogenized sample. The A(Li) versus $T_{\rm eff}$ trend cannot be eliminated without *very* major revisions of stellar models and calibrations. The metallicity dependence of A(Li), though significant according to statistical tests of these data, might conceivably be reduced or even eliminated through future systematic revisions of stellar atmosphere models, for example, if metallicity-dependent convection is found to be appropriate and if it has the required systematics to compensate for the currently observed trends. The persistence of these trends contradicts the findings of Molaro et al. (1995), but we argue that the inclusion of subgiants in their sample, which we regard as inappropriate, drove their result. We, on the other hand, reject subgiants since they had higher effective temperatures when they were on the main sequence themselves, and they have different evolutionary histories than the dwarfs now on the main sequence. Dwarfs and subgiants are astrophysically different and do not belong in the same sample for the investigation of these astrophysical trends.

We find that these correlations persist, but several points are worth noting: (*a*) suspected subgiants should be eliminated from the sample prior to conducting a regression analysis; (*b*) metallicity trends are evident only when stars of a wide range of metal abundances are included in the samples, especially the most metal-poor stars, (*c*) the tests must be performed in a multiple-regression environment (i.e., not when $T_{\rm eff}$ or [Fe/H] is considered the only independent variable), and (*d*) the results survive when regression methods resistant to the presence of high-leverage outliers are applied. Our current best estimate of Li abundance as a function of $T_{\rm eff}$ and [Fe/H], based on the full, homogenized sample A ($T_{\rm eff} > 5500$ K, [Fe/H] ≤ -1.2) analyzed with the resistant RLS/LMS technique is

$$A(\mathrm{Li}) = -0.09(\pm 0.30) + 0.0408(\pm 0.0052)T_{\rm eff}/100 + 0.111(\pm 0.018)[\mathrm{Fe/H}] .$$

The slopes of this relationship are consistent, within expected errors, with the results of Thorburn (1994), who considered the existence of a multiple correlation of A(Li) with $T_{\rm eff}$ and [Fe/H], and with the results of Norris et al. (1994) for an inhomogeneous sample which they divided into subsamples restricted by metallicity. The value of the constant in the fit, and to a lesser degree the other coefficients, is rooted in the choice of Bell (1981) models and the color–effective temperature transformations discussed in the text. The use of Balmer temperatures appears unlikely to significantly diminish the reported correlations, in contradiction to the claim of Molaro et al. (1995).

We reach the same finding as in our preliminary investigations (Deliyannis et al. 1992; Ryan 1993) and as Thorburn (1994) and Chaboyer & Demarque (1994), that the signature expected of uninhibited diffusion based on current models is not obvious in warm halo dwarfs, and we set an upper limit of order 0.1 dex on the amount of surface Li which has been removed by diffusion compared to nondiffusive models. The inclusion of rotation provides one means by which models may overcome diffusion, at the same time depleting Li from considerably higher values and acquiring a *range* of final Li abundances for similar atmospheric parameters; however, present

[9] Norris et al. (1994) noted that the spread of Li abundances toward lower values appeared to be greater below [Fe/H] = −3.0.

models of this type (e.g., Chaboyer & Demarque 1994) also currently fail to fit the observations adequately.

For stars with multiple observations, we compared equivalent width measurements with errors estimated on the basis of S/N and resolution, and we found in most cases very good agreement, with precisions of a few mÅ. However, we also identified a few cases in which the spread in Li equivalent width measurements exceeded these error estimates. Since accidental large errors like these possibly also exist among stars with only single observations, these can contribute additional scatter about the Spite plateau, which is used as a diagnostic to check for intrinsic spread in Li abundances. We defer our main discussion of the evidence concerning a spread to a subsequent paper, but we do note the existence of cases of well-observed stars with similar temperatures and metallicities which cannot have the same Li abundance. The contrast between G64−12, G64−37, and CD −33°1173 provides an example of such stars, all having [Fe/H] < −3.0 where Norris et al. (1994) saw an increase in the spread of Li abundances toward generally lower values.

The authors are grateful to the Canada-France-Hawaii Telescope for providing facilities for this study, and to an anonymous referee for suggestions on improving the manuscript. S. G. R. is grateful for support from D. A. VandenBerg under his operating grant awarded by the Natural Science and Engineering Research Council of Canada and later from the Australian Research Council. T. C. B. acknowledges partial support for this work from an All University Research Initiation Grant awarded by Michigan State University, and from grants AST 90-1376 and AST 92-22326 awarded by the National Science Foundation. C. P. D. gratefully acknowledges support for this work provided by NASA through grants NAGW-777 and NAGW-778 to Yale University, by the University of Hawaii Foundation, and by NASA through grant HF-1042.01-93A awarded by the Space Telescope Science Institute, which is operated by the Association of Universities for Research in Astronomy, Inc., for NASA under contract NAS 5-26555. Similarly, J. A. T. acknowledges support from NASA grant HF-1064.01-94A awarded by the Space Telescope Science Institute.

REFERENCES

Bell, R. A. 1981, private communication
Bell, R. A., & Oke, J. B. 1986, ApJ, 307, 253
Bessell, M. S. 1979, PASP, 91, 589
Bevington, P. R. 1969, Data Reduction and Error Analysis for the Physical Sciences (New York: McGraw–Hill)
Boesgaard, A. M. 1985, PASP, 97, 784
———. 1991, in ASP Conf. Ser. 13, The Formation and Evolution of Star Clusters, ed. K. Janes (Provo: ASP), 463
Buser, R., & Kurucz, R. L. 1992, A&A, 264, 557
Carlsson, M., Rutten, R. J., Bruls, J. H. M. J., & Shchukina, N. G. 1994, A&A, 288, 860
Carney, B. W. 1979, ApJ, 233, 211
———. 1989, private communication
Carney, B. W., Latham, D. W., Laird, J. B., & Aguilar, L. A. 1994, AJ, 107, 2240
Cayrel, R. 1988, in The Impact of Very High S/N Spectroscopy on Stellar Physics, ed. G. Cayrel de Strobel & M. Spite (Dordrecht: Kluwer), 345
Cayrel de Strobel, G., Hauck, B., Francois, P., Thevenin, F., Friel, E., Mermilliod, M., & Borde, S. 1992, A&AS, 95, 273
Chaboyer, B., Deliyannis, C. P., Demarque, P., Pinsonneault, M. H., & Sarajedini, A, 1992, ApJ, 388, 372
Chaboyer, B., & Demarque, P. 1994, ApJ, 433, 510
Deliyannis, C. P. 1990, Ph.D. thesis, Yale Univ.
Deliyannis, C. P., Beers, T. C., & Ryan, S. G. 1992, BAAS, 24, 1278
Deliyannis, C. P., Boesgaard, A. M., King, J. R., & Duncan, D. K. 1995, preprint
Deliyannis, C. P., & Demarque, P. 1991, ApJ, 379, 216
Deliyannis, C. P., Demarque, P., & Kawaler, S. D. 1990, ApJS, 73, 21
Deliyannis, C. P., Pinsonneault, M. H., & Duncan, D. 1993, ApJ, 414, 740
Demarque, P., Deliyannis, C. P., & Sarajedini, A. 1991, in Observational Tests of Inflation, ed. T. Shanks et al. (Dordrecht: Kluwer), 111
Fields, B. D., Olive, K. A., & Schramm, D. N. 1994, ApJ, 435, 185
Hobbs, L. M., & Duncan, D. K. 1987, ApJ, 317, 796
Hobbs, L. M., & Pilachowski, C. 1988, ApJ, 326, L23
Hobbs, L. M., & Thorburn, J. A. 1991, ApJ, 375, 116
———. 1994, ApJ, 428, L25
Hobbs, L. M., Welty, D. E., & Thorburn, J. A. 1991, ApJ, 373, L47
King, J. R. 1993, AJ, 106, 1206
Kurucz, R. L. 1989, private communication
———. 1993, CDROM-13 (Cambridge: SAO)
———. 1995, ApJ, 452, 102
Magain, P. 1987, A&A, 181, 323
Michaud, G. 1970, ApJ, 160, 641
Molaro, P., Primas, F., & Bonifacio, P. 1995, A&A, 295, L47
Norris, J. E., Ryan, S. G., & Stringfellow, G. S. 1994, ApJ, 423, 386
Pilachowski, C. A., Hobbs, L. M., & De Young, D. S. 1989, ApJ, 345, L39
Pilachowski, C. A., Sneden, C., & Booth, J. 1993, ApJ, 407, 699
Pinsonneault, M. H., Deliyannis, C. P., & Demarque, P. 1992, ApJS, 78, 181
Prantzos, N., Casse, M., & Vangioni-Flam, E. 1993, ApJ, 403, 630
Proffitt, C. R., & Michaud, G. 1991, ApJ, 371, 584
Proffitt, C. R., & VandenBerg, D. A. 1991, ApJS, 77, 473
Rebolo, R., Beckman, J. E., & Molaro, P. 1987, A&A, 172, L17
Rebolo, R., Molaro, P., & Beckman, J. E. 1988, A&A, 192, 192
Rousseeuw, P. J., & Leroy, A. M. 1987, Robust Regression & Outlier Detection (New York: Wiley)
Ryan, S. G. 1989, AJ, 98, 1693
———. 1993, in Origin and Evolution of the Elements, ed. S. Kubono & T. Kajino (Singapore: World Scientific), 3
Ryan, S. G. Norris, J. E., Bessell, M. S., & Deliyannis, C. P. 1992, ApJ, 388, 184
Schuster, W. J., & Nissen, P. E. 1988, A&AS, 73, 225
———. 1989, A&A, 222, 69
Schuster, W. J., Parrao, L., & Contreras Martinez, M. E. 1993, A&AS, 97, 951
Spite, F., & Spite, M. 1982, A&A, 115, 357
———. 1986, A&A, 163, 140
———. 1993, A&A, 279, L9
Spite, M., Maillard, J. P., & Spite, F. 1984, A&A, 141, 56
Spite, M., Spite, F., Peterson, R. C., & Chaffee, F. C. 1987, A&A, 172, L9
Tayler, R. J. 1986, MNRAS, 220, 793
Thorburn, J. A. 1992, ApJ, 399, L83
———. 1994, ApJ, 421, 318
Thorburn, J. A., & Beers, T. C. 1993, ApJ, 404, L13
VandenBerg, D. A., & Bell, R. A. 1985, ApJS, 58, 561